# A survey of icephobic coatings and their potential use in a hybrid coating/active ice protection system for aerospace applications

Xiao Huang, Nick Tepylo, Valérie Pommier-Budinger, Marc Budinger, Elmar Bonaccurso, Philippe Villedieu, Lokman Bennani

▶ **To cite this version:**

Xiao Huang, Nick Tepylo, Valérie Pommier-Budinger, Marc Budinger, Elmar Bonaccurso, et al.. A survey of icephobic coatings and their potential use in a hybrid coating/active ice protection system for aerospace applications. Progress in Aerospace Sciences, 2019, 105, pp.74-97. 10.1016/j.paerosci.2019.01.002 . hal-02024879

**HAL Id: hal-02024879**
**https://hal.science/hal-02024879**

Submitted on 19 Feb 2019

**HAL** is a multi-disciplinary open access archive for the deposit and dissemination of scientific research documents, whether they are published or not. The documents may come from teaching and research institutions in France or abroad, or from public or private research centers.

L'archive ouverte pluridisciplinaire **HAL**, est destinée au dépôt et à la diffusion de documents scientifiques de niveau recherche, publiés ou non, émanant des établissements d'enseignement et de recherche français ou étrangers, des laboratoires publics ou privés.


# Open Archive Toulouse Archive Ouverte (OATAO)

OATAO is an open access repository that collects the work of some Toulouse researchers and makes it freely available over the web where possible.

This is an author's version published in: https://oatao.univ-toulouse.fr/22835

**Official URL**: https://doi.org/10.1016/j.paerosci.2019.01.002

**To cite this version :**

Huang, Xiao and Tepylo, Nick and Pommier-Budinger, Valérie and Budinger, Marc and Bonaccurso, Elmar and Villedieu, Philippe and Bennani, Lokman A survey of icephobic coatings and their potential use in a hybrid coating/active ice protection system for aerospace applications. (2019) Progress in Aerospace Sciences, 105. 74-97. ISSN 0376-0421

Any correspondence concerning this service should be sent to the repository administrator: tech-oatao@listes-diff.inp-toulouse.fr

# A survey of icephobic coatings and their potential use in a hybrid coating/active ice protection system for aerospace applications

Xiao Huang[a], Nick Tepylo[a,*], Valérie Pommier-Budinger[b], Marc Budinger[c], Elmar Bonaccurso[d], Philippe Villedieu[e], Lokman Bennani[e]

[a] Department of Mechanical and Aerospace Engineering, Carleton University, 1125 Colonel By Drive, K1S 5B6, Ottawa, ON, Canada
[b] ISAE-SUPAERO, Université de Toulouse, 31400 Toulouse, France
[c] Institut Clément Ader, Université de Toulouse, INSA, ISAE-SUPAERO, MINES, ALBI, UPS, CNRS, 31400 Toulouse, France
[d] AIRBUS Central R&T, XRXG, 81663, Munich, Germany
[e] Department of Multiphysics for Energetic, ONERA, 2 Avenue Edouard Belin, 31500 Toulouse, France

*Keywords:*
Icephobic coating
De-icing
Anti-icing
Ice adhesion
Hybrid ice protection system
Electro-mechanical de-icing

A B S T R A C T

Icephobic coatings for aircraft and other surfaces subjected to ice accretion have generated great interest in the past two decades, due to the advancement of nanomaterials, coating fabrication methods, biomimetics, and a more in-depth understanding of ice nucleation and ice adhesion. Icephobic coatings have demonstrated the ability to repel water droplets, delay ice nucleation and significantly reduce ice adhesion. Despite these ongoing research activities and promising results, the findings reported hereafter suggest that coatings alone cannot be used for aircraft anti-icing and de-icing operations; rather, they should be considered as a complementary option to either thermal or mechanical ice protection methods, for reducing power consumption and the ecological footprint of these active systems and for expediting ground de-icing operations. This paper will first review the state-of-the-art of icephobic coatings for various applications, including their performance and existing deficiencies. The second part of this paper focuses on aerospace anti-icing and de-icing requirements and the need for hybrid systems to provide a complete ice protection solution. Lastly, several urgent issues facing further development in the field are discussed.

## 1. Introduction

Ice accretion on aircraft has an adverse impact on both safety and performance [1]. As such, there have been great efforts devoted to the development of strategies for de icing and anti icing. “De icing” refers to the removal of ice from aircraft surfaces and its methods include heating, vibration (contact or non contact), mechanical means (e.g., inflated boots on aircraft leading edges) and sprayed icing fluids [2] to remove any ice accretion, while “anti icing” is a preventive measure that delays or reduces ice accretion on surfaces so that the subsequent de icing process is not needed or less time/energy will be needed during de icing. Anti icing can be achieved by frequent spraying of anti freezing fluids or by the application of permanent coatings (hydro phobic or icephobic), designed to prevent water droplets from adhering to the surface before freezing, to delay the freezing event, and/or to reduce ice adhesion to the surface [3]. The use of de icing fluids for de icing and anti icing purposes has a severe environmental impact [4,5], while a permanent, long lasting coating can lessen such consequence.

The development of icephobic surfaces can be dated back to the late 1950s [6,7]. However, due to the complexity of icing conditions and ice interaction with surfaces, there has not been a proven, commercially viable (low cost, easy application) and durable (repeated icing/de icing cycles, surface abrasion and mechanical loading) icephobic coating for aerospace applications thus far. Some promising coatings have shown to be able to reduce ice adhesion up to several orders of magnitude with respect to reference metal surfaces such as aluminium, titanium or steel, while others could delay ice crystal nucleation from supercooled water droplets or humid air for up to several hours. The purpose of this paper is to first briefly provide an overview of the aircraft ice accretion process and then summarize the latest icephobic coatings and their performance. The second part of the paper focuses on the requirements for effective aircraft anti icing and de icing strategies. Based on the

* Corresponding author.
*E-mail addresses:* Xiao.huang@carleton.ca (X. Huang), nick.tepylo@carleton.ca (N. Tepylo), valerie.budinger@isae-supaero.fr (V. Pommier-Budinger), marc.budinger@insa-toulouse.fr (M. Budinger), elmar.bonaccurso@airbus.com (E. Bonaccurso), Philippe.Villedieu@onera.fr (P. Villedieu), Lokman.Bennani@onera.fr (L. Bennani).

https://doi.org/10.1016/j.paerosci.2019.01.002

**List of abbreviations**

| | |
|---|---|
| AIAA | American Institute of Aeronautics and Astronautics |
| Al | aluminium |
| AMIL | Anti icing Materials International Laboratory |
| ARF | adhesion reduction factor |
| ASME | American Society of Mechanical Engineers |
| ASTM | American Society for Testing and Materials |
| CA | contact angle |
| CAH | contact angle hysteresis |
| CFRP | carbon fibre reinforced polymer |
| CNT | carbon nanotube |
| CVD | chemical vapour deposition |
| DLC | diamond like carbon |
| DoE | design of experiments |
| DRIE | deep reactive ion etching |
| EIDI | electro impulsive de icing systems |
| EMED | electro mechanical expulsive de icing systems |
| ETIPS | electro thermal ice protection systems |
| FAR | Federal Aviation Regulations |
| FETS | perfluorodecyltrichlorosilane |
| FOTS | fluorooctyltrichlorosilane |
| FPD | freezing point depressant |
| FPU | fluorinated polyurethane |
| GFRP | glass fibre reinforced polymer |
| GNRs | graphene nanoribbons |
| HDFS | heptadecafluoro 1,1,2,2 tetrahydrodecyl trichlorosilane |
| ICTS | icing contaminated tail stall |
| IPS | ice protection system |
| IWTT | icing wind tunnel tests |
| LWC | liquid water content |
| MVD | mean effective droplet diameter |
| OEM | original equipment manufacturer |
| PAA | phosphoric acid anodizing |
| PDMS | polydimethylsiloxane |
| PECVD | plasma enhanced chemical vapour deposition |
| PFPE | polyfluorinated polyether |
| PTFE | polytetrafluoroethylene |
| PU | polyurethane |
| PVD | physical vapour deposition |
| PVDF | polyvinylidene fluoride |
| REACH | Registration, Evaluation, Authorisation and Restriction of Chemicals |
| RoA | roll off angle |
| RTV | room temperature vulcanizing |
| SA | stearic acid |
| SAA | sulphuric acid anodizing |
| SAE | Society of Automotive Engineers |
| SAM | surface assembled monolayer |
| SEM | scanning electron microscopy |
| SLDs | supercooled large droplets |
| SLIPS | Slippery Liquid Infused Porous Surfaces |
| SMA | shape memory alloy |
| TAT | total air temperature |
| Ti | titanium |
| TiAlN | titanium aluminium nitride |
| TiN | titanium nitride |
| UV | ultraviolet |

state of the art technologies, future development in combining active systems and engineered coating materials into a hybrid system are proposed.

## 2. Aircraft de-icing and anti-icing methods

### 2.1. Ice formation and accretion on aircraft

Ice accretion on aircraft during flight can either be caused by impinging supercooled water droplets, freezing rain, or snow particulates accumulating on the surface. The most common of these are supercooled water droplets which typically have a mean effective droplet diameter (MVD) less than 50 microns. The droplets impact the surface and can freeze on contact near the stagnation point or can roll back along the wing and freeze. Water can also exist in supercooled large droplets (SLDs) (typically larger than 50 μm) that freeze upon contact and the release of their latent heat melts them back into the liquid phase where they refreeze further back on the aircraft [8,9]. In addition to droplet size, atmospheric conditions, airfoil geometry, aircraft velocity and angle of attack all together contribute to the formation and coverage of ice [10]. Ice accretion commonly occurs on the upper and lower wing surfaces, fuselage, propellers, engine nacelles, radomes and sensor ports as shown in Fig. 1. In addition to the general performance reduction, the adverse effects of icing on aircraft include wing stall, icing contaminated tail stall (ICTS), icing contaminated roll upset, engine and air intake icing, carburetor icing, propeller icing, static and dynamic port blockage, probe icing and windshield icing.

There are three types of ice that can form in flight; rime, glaze, and mixed ice. Rime ice consists of mostly frozen supercooled water droplets and forms at low temperatures in stratiform clouds while glaze ice (partially frozen supercooled water droplets) forms just below the freezing temperature of water in mostly cumulus type clouds as outlined in Fig. 2. Mixed ice forms in the middle of the freezing range which usually is between 0 and −20 °C (−40 °C in extreme conditions) [11]. Glaze ice can be difficult to remove as the supercooled water droplets exist mostly in the liquid state and are thus mobile once they contact the surface. The water droplets are able to coalesce, forming a sheet with a continuous bond to the surface. Since rime ice is generated from smaller droplets, they are unable to coalesce and as a result, freeze in place.

It was qualitatively determined that hydrophobic coatings can be more effective in glaze ice conditions than icephobic coatings under rime conditions [12]. The concentration and distribution of the supercooled water droplets and ice crystals inside the cloud vary with

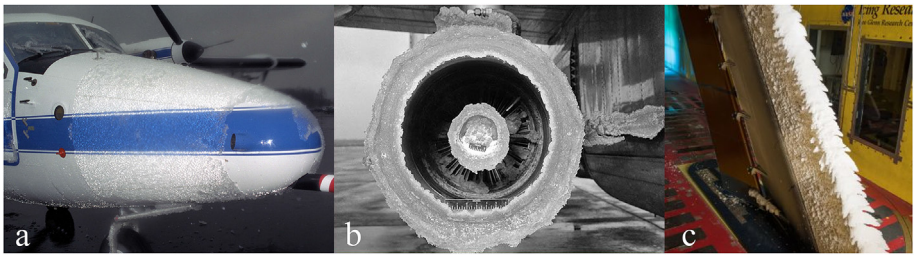


**Fig. 1.** Ice accretion on (a) aircraft fuselage, (b) engine inlet and (c) aircraft surface. All images supplied by NASA [126].

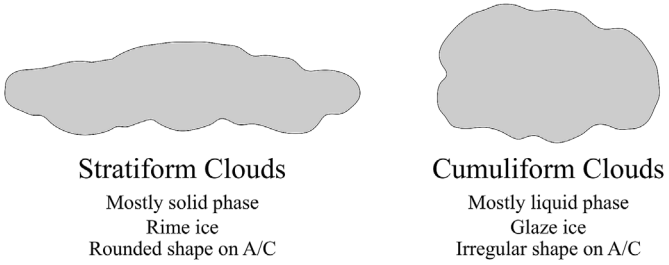


**Fig. 2.** Ice characteristics for stratiform and cumuliform clouds.

temperature and altitude as shown in Fig. 3. As the temperature decreases, so does the saturated vapor density (the amount of water vapour the air can hold) while the probability of the droplets freezing increases, leading to a reduced icing probability. The ice accumulation rate is also related to the amount of supercooled water inside the cloud, where the highest amount of ice accretion would occur at temperatures just below the freezing point. Severe icing can also occur below the cloud level in freezing rain conditions.

Hoar frost, another form of ice, forms on the aircraft on the ground or in flight when descending from below freezing condition to an altitude with warm and moist air. Frost accumulation on the surface can impact aircraft performance and visibility. It is more prone to form in areas with more surface asperities. i.e., rough surfaces. Snow, on the other hand, is a mixture of ice and water and its accumulation commonly occurs on the ground.

Frost, ice, and snow can also accumulate on aircraft surfaces while on the ground. If not removed, this accretion can reduce the lift by up to 30% and increase drag by 40% [13]. All five types of ice/snow accumulation on aircraft are classified as “dangerous” to air traffic [1].

### 2.2. De icing and anti icing methods

Various ice protection systems (IPS) can be employed to protect aircraft surfaces, engine inlets, sensors and windshields from ice accumulation in flight and on the ground. A summary of both existing and potential methods and their applications are provided in Table 1 and Table 2.

### 2.3. FAA certificated vs. non hazard

For flight certification, the FAA calls for a 45 min hold pattern during flight in continuous, maximum icing conditions found in stratus clouds without the use of an ice protection system [14]. Unprotected surfaces to be tested include: landing gear, antennas, fuselage nose cones or radomes, fuel tank vents, fuel tip tanks, and the leading edge of control surfaces. A non hazard de icing or anti icing system should only be considered as a way for immediate escape from icing conditions. The non hazard de icing systems installed are not to be tested for performance in icing conditions, rather they must show that in dry air, the installation of various systems does not adversely affect performance, stability, and other flight characteristics. Due to this loose certification standard, these systems are considered non essential to the aircraft. For many of the coating systems discussed throughout this review, if they are to be used as FAA certified passive anti icing and de icing measures, rigorous tests must be conducted under the conditions stipulated in FAA certification once other standard tests have been carried out per customer specifications.

## 3. Icephobic coating development

### 3.1. Hydrophobic/superhydrophobic vs. icephobic

Icephobicity and hydrophobicity have been considered closely related and many icephobic coatings were in fact derived from hydrophobic or superhydrophobic coatings and surface processing methods. Although a standard definition of icephobicity has not yet been agreed upon, an extensive body of work exists in the field of hydrophobic and superhydrophobic coatings. A brief overview of these surfaces is provided here. A more detailed, all encompassing review of this subject can be found in Ref. [15].

A surface is classified as hydrophobic when the water contact angle (CA) on this surface is $> 90°$; while a superhydrophobic surface has a water contact angle $> 150°$ and a contact angle hysteresis (CAH) $< 10°$ [16]. CAH is defined as the difference between the advancing and the receding CA of a water droplet that expands or shrinks on surface. Alternatively, the roll off angle (RoA) can be determined as the lowest angle a surface needs to be inclined before a water droplet rolls or slides off it. Superhydrophobic surfaces should also exhibit RoA $< 10°$ [17]. These definitions are illustrated in Fig. 4.

Superhydrophobic coatings, most of which mimic the surface microstructure of water repellent plants or leaves, have been viewed historically as potential icephobic coatings in that they offer the advantage of reducing ice adhesion or accretion from supercooled water sprayed or poured onto the surface [18 20] (see Fig. 5). This was based on the reasoning that water and ice have a similar surface tension/surface energy and that a surface that repels water should have the ability to prevent ice accretion as well.

Although superhydrophobic coatings have been investigated as part of an aircraft ice protection system [21], there are no studies conducted at aircraft cruise velocities ($> 75$ m/s) as noted by Yeong et al. [22] who recently performed tests in an icing wind tunnel at speed 50 and 70 m/s. Most of these studies use droplet impact velocities below 10 m/s [23,24] or freezing conditions not in line with typical aircraft icing conditions [25,26]. In early work conducted on bare aircraft substrates, Scavuzzo and Chu demonstrated that the ice adhesion strength increases with impact velocity [27]. In a similar study conducted on superhydrophobic coatings, it was shown that the effectiveness of the coating decreased by increasing either the MVD or LWC [28]. Larger droplets have more momentum and thus are able to penetrate deeper into the surface asperities, increasing the effective contact area and the ice adhesion strength. Increases in the LWC promote frost formation which increases ice adhesion. Yeong et al. [22] obtained results at relatively high speed by generating rime and glaze ice on samples at 50 and 70 m/s with 20 micron MVD droplets. They showed that increasing droplet impact speeds tend to decrease the effectiveness of superhydrophobic coatings. They also found that the 20 micron MVD droplets penetrate into the surface asperities and that the maximum

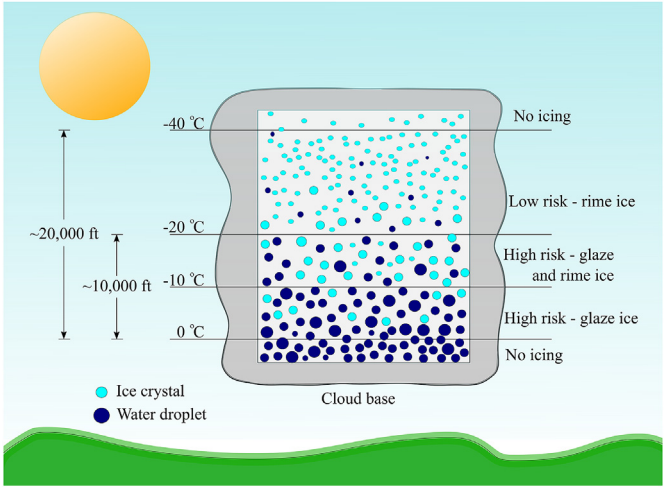


**Fig. 3.** Ice formation within a cloud and the resulting probability of aircraft icing.

**Table 1**
In-flight de-icing and anti-icing methods on aircraft (summarized from Refs. [13,14,117,130,131]).

| Method | Description of Technology | De-icing Potential | Anti-icing Potential | Advantages and Disadvantages |
|---|---|---|---|---|
| Freezing point depressants (FPD) (e.g., glycol) | - Ice removed by pumping FPD through porous outer skin in-flight and spraying heated FPD on the ground<br>- If a thin layer of FPD is remains on the aircraft surface, short-term anti-icing can be achieved | Yes | Yes | - Can be used on the ground and in-flight<br>- Layer of FPD on the aircraft can result in detrimental effects to aircraft performance<br>- Fluids can be toxic and cause environment concerns |
| Engine bleed air | - Hot engine air redirected to the leading edge, heating the surface and melting the accreted ice<br>- If no ice is present, it can prevent droplets from freezing and evaporate droplets on the surface | Yes | Yes | - Reduction in engine efficiency<br>- Not available on piston and turboprop-powered airplanes<br>- High system weight due to required internal piping |
| Electro-thermal (embedded heaters) | - Heating coils placed in the leading edge can melt accumulated ice when supplied with electrical energy<br>- Can prevent the impinging droplets from freezing | Yes | Yes | - Large power consumption, about 1.5–2 $W/cm^2$<br>- Limited to critical areas<br>- Surfaces must be thermally conductive |
| Pneumatic boots | - Rubber boots installed on the leading edge inflate with air to break accumulated ice into chunks | Yes | No | - Rubber boots become rigid at low temperatures limiting effectiveness to temperatures $>$ -20 °C<br>- Require frequent dressing and inspection<br>- Aerodynamic performance degradation when deployed |
| Pneumatic impulse | - Rubber boots are embedded in a metal or polymer system on the outside of the leading edge<br>- When inflated, the boots expand rapidly, expelling any ice build-up | Yes | No | - Protective layers consisting of metal or polymers are required to prevent the tubes from being exposed to rain erosion, ice pellet impingement and other forms of surface damage<br>- Can remove ice at temperatures as low as $-55$ °C |
| Electro-impulse | - High-voltage capacitors on the inside of the leading edge are rapidly discharged which generates an electromagnetic repulsive force in the skin causing fracture of ice bonded to the surface | Yes | No | - Used to de-ice power transmission lines<br>- May cause electromagnetic interference with other aircraft systems components<br>- Can cause structural fatigue<br>- No longer in use for aerospace |
| Electro-expulsive separation system | - Magnetic fields are generated about the two parallel layers of conductors, producing forces that push the conductors apart. When current is passed into the system, the rapid acceleration of the conductors breaks the bond the ice has formed with the surface | Yes | No | - Short response time (ms)<br>- Low power consumption (Tested on Cessna Skymaster and installed on Raytheon business jet) |
| Shape memory alloys (SMA) | - SMAs (e.g., NiTi) can change shape when heat is applied. If ice is present, the heat will cause the leading edge erosion shield to deform to a predefined shape, expelling the ice | Yes | No | - Only for leading edge erosion shields<br>- Energy required is dependent on the surface temperature<br>- Drag increase may be significant when deformed and during the return to its original shape |
| Ultrasound technology [132] | - When supplied with current, piezoelectric actuators on the inside of the leading edge produce ultrasonic waves that travel through the aircraft skin, generating shear stresses at interface between the ice and surface. These shear stresses debond and break apart the ice layer | Yes | Yes | - Piezoelectric actuators require a lower power density than other methods for ice delamination<br>- Actuator count required based on the size of surface needing protection<br>- Bond strength to the surface may be fatigued after billions of cycles |
| Microwave [131] | - Microwave energy transferred through aircraft leading edge and converted to heat which melts the bond that ice has formed with the surface | Yes | Yes | - Intended for use on turboprop aircraft<br>- Can cause interference with other electronics<br>- More energy intensive than other systems |

**Table 2**
Anti-icing and de-icing methods used on different parts of aircraft [13].

| Component | Turbo-jet | Propeller-driven aircraft | Issues with potential use of coatings in combination with the already existing method of de-icing |
|---|---|---|---|
| Airfoil leading edges | - Engine bleed air<br>- Pneumatic boots<br>- Porous fluid panel | - Pneumatic boots<br>- Porous fluid panel | - Polymer coating will need to be heat conductive<br>- Anti-icing coatings on boots may be a viable choice, if flexible<br>- Application of coatings on perforated surface may be challenging |
| Engine air intakes | - Engine bleed air<br>- Pneumatic boots<br>- Electrical heater mats | - Engine bleed air<br>- Pneumatic boots<br>- Electrical heater mats | - Similar to above<br>- Similar to above<br>- Heating mats may be incorporated into the coating to reduce power consumption for de-icing |
| Propellers | | - Electric heater mats<br>- Fluid systems | -Similar to above -Advantageous if combined with a liquid infused coating system |
| Windshields | - Electrical heaters | - Electrical heaters | - Similar to above |
| Pitot-static systems | - Electrical heaters | - Electrical heaters | - Similar to above |
| Probes and drain masts | - Electrical heaters | - Electrical heaters | - Similar to above |
| Control surface horns | - Electrical heater mats | - Electrical heater mats | - Similar to above |

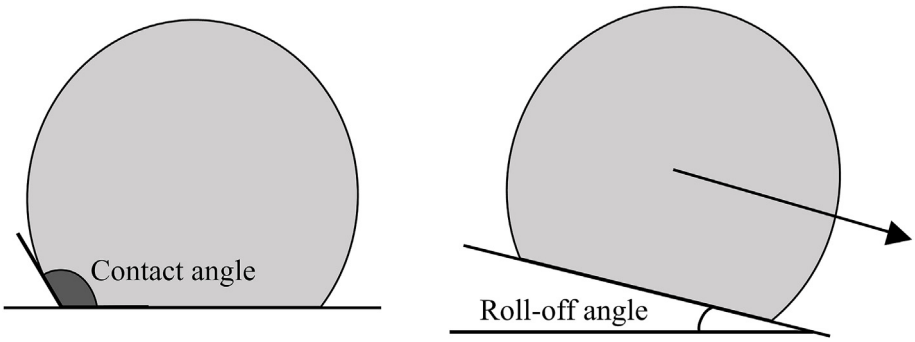


**Fig. 4.** The contact angle and roll-off angle of a water droplet.

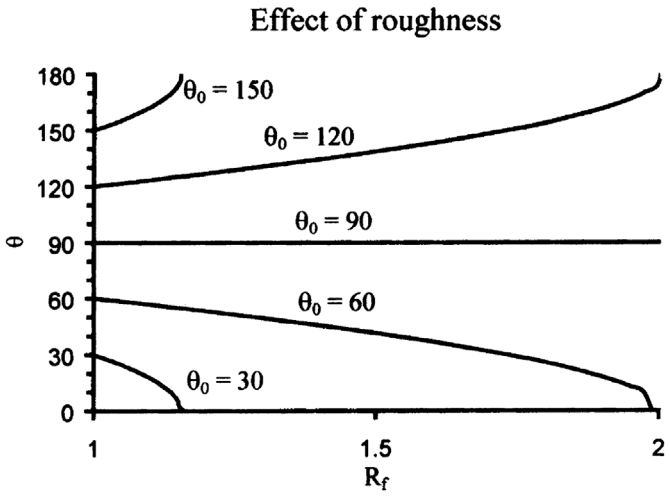


**Fig. 5.** Contact angle as a function of roughness factor (r = actual surface area/geometric surface area) for different smooth surfaces of different CA. Reproduced from Ref. [127] with permission from Springer Nature.

roughness height to prevent this was approximately 10 nm. All these results appear to be significant obstacles for the field of super hydrophobic coating development.

In addition, the water repellent ability of micro textured super hydrophobic surfaces may be compromised, or even reversed (to hy drophilic) under frost forming conditions. In fact, frost can also form on micro textured superhydrophobic surfaces, which are water repellent only to liquid water drops and not to condensed water microdroplets. Once a frost layer is formed on the surface, the surface turns into a hydrophilic surface. Frost formation commonly occurs on the surface of many outdoor structures such as wind turbine blades, power lines, communication towers and aircraft on the ground. During flight, ice accretion is usually due to supercooled water droplets impinging on aircraft surfaces.

The icephobicity of a surface not only depends on intrinsic surface properties, but also on the ice formation conditions. In a reported study of a surface with an array of hydrophobic silicon posts (Fig. 6), which was demonstrated to be a superhydrophobic surface for sessile water drops, the cooled surface frosted more readily under high humidity [18]. As a result, superhydrophobicity was lost, (the surface turned hydrophilic) due to the frost layer, and the increased effective surface area led to a higher ice adhesion strength when compared with smooth surfaces. In addition to experimental studies, theoretical force balance analysis also revealed that superhydrophobic surfaces were not ne cessarily icephobic [29]. As such, under different icing conditions, su perhydrophobicity does not always directly translate into icephobicity [30,31], particularly if the surface structure is not specifically tailored to prevent frost formation. On the other hand, ice adhesion on non micro textured surfaces decreases as hydrophobicity increases [32,33].

### *3.2. General coating classification and requirements*

Icephobic coatings can be classified based on their chemical com positions, surface topology and application methods. Polymer or com posite coatings in the forms of “paints”, that can be applied employing standard a spray, dip, brush, or an electrostatic deposition process, are beneficial for large structures such as aircraft and wind turbine blades. In contrast, coatings applied by either physical or chemical vapour deposition (PVD/CVD) or ion milling are rather applicable to smaller and higher cost devices, as these processes are carried out in an en closed chamber and the equipment and process costs are higher. Coatings fabricated using these processes also have limited thickness, which makes them less resistant to extreme weather conditions (freezing rain, dust particles, or ice crystals). Currently, the most pro mising icephobic coatings are based on two coating design principles: surface micro and nano texturing followed by a chemical

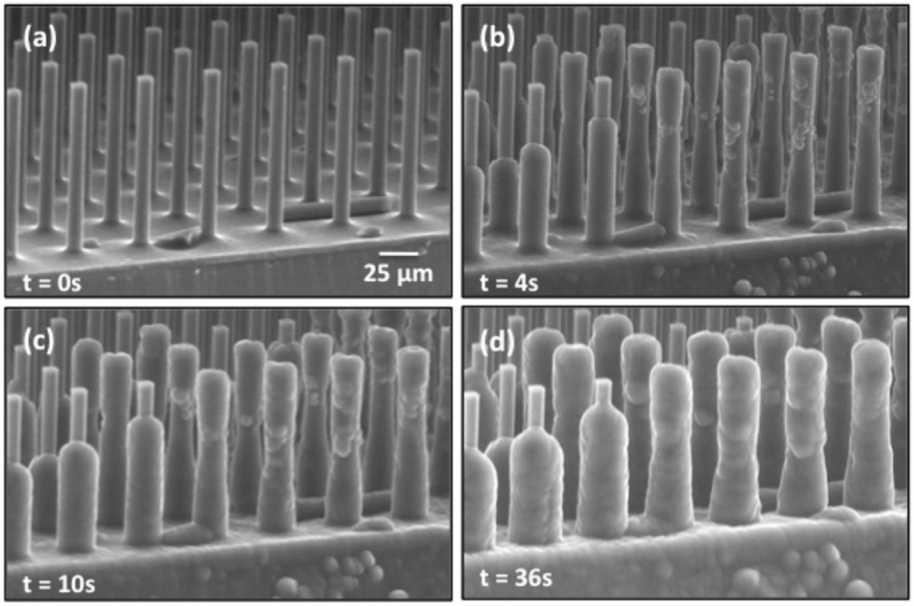


**Fig. 6.** Scanning electron microscopy (SEM) images illustrating gradual frost formation on a superhydrophobic surface within 36 s at 13 °C. Figures reproduced from Ref. [18] with permission from AIP.

functionalization (similar to superhydrophobic coatings based on the lotus leaf design) and infusing low surface energy polymeric matrices with functional lubricants (similar to slippery surfaces based on the *Nepenthes* pitcher plant design) [34].

For modelling ice adhesion to a smooth substrate, one can consider that the bonding strength on the atomic/molecular level depends upon three basic forces: electrostatic forces, covalent/chemical bonds, and van der Waals interactions [3]. The dielectric constant of a material affects the electrostatic attractive force; also, ice adhesion has been found to decrease with the dielectric constant of the surface material [35]. Teflon based materials have an inherently low dielectric constant ($\approx 2$) and are commonly used for hydrophobic and icephobic coating formulations. In fact, a RF sputtered Teflon showed almost negligible ice adhesion value when tested using a centrifugal ice adhesion appa ratus [36]. This shows that a low electrostatic force plays a significant role since van der Waals forces decay much more rapidly with distance than electrostatic forces. On the other hand, water (or ice), being a polar molecule with an exposed hydrogen atom, forms a strong bond with a substrate due to hydrogen bonding. The key to coating designs for reduced ice adhesion is to select materials with a low bonding strength to $H_2O$. The effects of hydrogen bonds on the interface bonding have been studied by many researchers [32,37,38]. Using a range of mixtures of zero hydrogen bonding with a hydrophobic surface as sembled monolayer (SAM) of 1 dodecanethiol and a surface with a hydrophilic nature like a SAM of 11 hydroxylundecane 1 thiol, ex perimentally determined ice adhesion values showed that hydrogen bonding was the greatest contributing factor to ice adhesion [38]. On a microscopic level, the ice adhesion strength to a substrate is also af fected by surface roughness, i.e., mechanical interlocking between the ice and substrate. The greater the surface roughness, the larger the mechanical adhesion is between the ice and substrate.

In summary, icephobic coatings can be designed by means of matrix compositions and topologies to achieve one or several of the following functions; these can also be used to define and compare icephobicity.

Detachment or removal of water droplets from a coated surface (ice droplets roll off surface before freezing).
Prevention or delay of ice formation via decreased heat transfer between impinging supercooled droplets and substrate so that ice crystallization is delayed.
Reduce the ice adhesion strength to the surface below 100 kPa so that minimum energy/force is needed for de icing (in a passive system, it was suggested that for a coating requires an ice adhesion strength below 20 kPa [39]).

In terms of ice adhesion strength, there exists a large variation in the published work for an individual substrate. This is in part due to the wide spectra of icing test conditions, ice thickness, the use of different adhesion test methods (lap shear, centrifuge, 0° cone test, bend test, knife edge test, impact [15,37]) and experimental variables. A review of the various testing methods and the measurements resulting from each test can be found in Ref. [40]. For example, the reported ice adhesion to an uncoated aluminium (Al) substrate ranges from 110 [29] to 1360 kPa [41]. As such, in many instances ice adhesion will be de scribed qualitatively by the adhesion reduction factor (ARF) or com paratively throughout this communication. The ARF is a comparison between the adhesion strength of the icephobic coating and a reference surface (typically aluminium). A high ARF ($> 10$) is characteristic of an icephobic coating. Throughout the following sections on coatings, the durability in the form of resistance to mechanical and chemical attack will be commented, whenever such information is available.

### 3.3. Icephobic coatings and properties

There are several categories of icephobic coatings (illustrated in Fig. 7) that will be outlined throughout this section. Ice adhesion strengths are reported; however, they may not be directly comparable due to the different physical test setups and selected parameters.

#### 3.3.1. Polymer coatings based on fluoropolymers

Polytetrafluoroethylene (PTFE, commercially known as Teflon) bulk material, PTFE films, and fluorinated silicone rubber/polyurethane coatings were investigated to understand the effects of chemical com position and surface roughness on ice adhesion [42]. In one study, PTFE coatings were applied to aluminium substrates by a spray and sintering method (the sintering temperature of 350 370 °C is high for a fully heat treated aged hardened aluminium alloy). The fluorinated coatings were applied by spraying and curing. The highest water contact angle, 152.8°, was recorded on one of the sintered PTFE surfaces. The sub micron grain structures, with gaps smaller than the mean water droplet

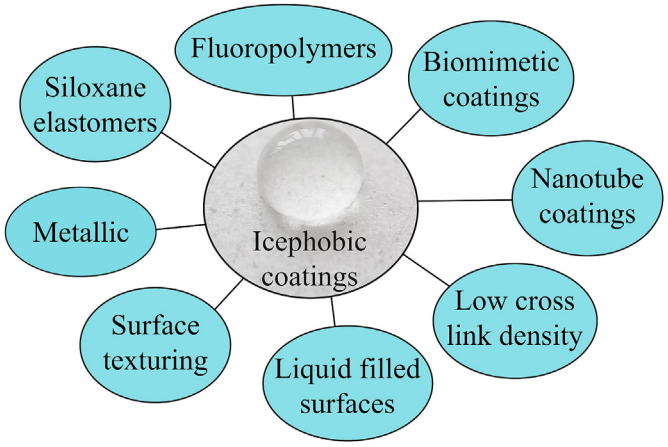


**Fig. 7.** Schematic of the different categories of icephobic coatings.

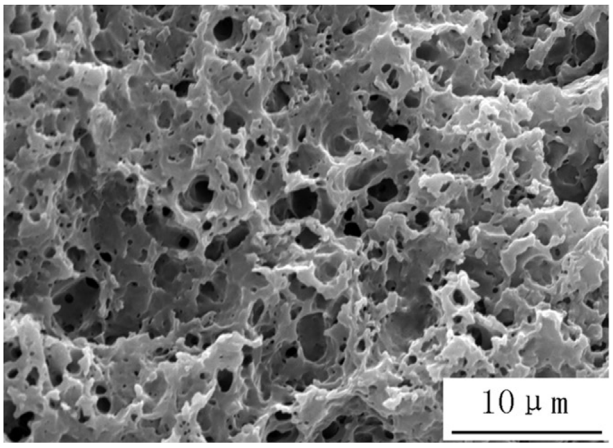


**Fig. 9.** Image of PVDF porous coating reproduced from Ref. [43] with permission from Elsevier.

sizes, effectively trapped air and enabled a Cassie Baxter state of water on the PTFE surface as shown in Fig. 8. The two images illustrate the different surface morphologies that resulted from the use of different raw powder material. The ice adhesion test, however, showed that both sintered PTFE coatings had very large ice adhesion strength under shear (1560 and 1820 kPa for the rod and spherical particles, Fig. 8 a and b). In contrast, the smooth bulk PTFE has the lowest ice bonding strength (60 kPa). In another study, polyfluorinated polyether (PFPE) dip coating was able to reduce ice adhesion of a bare aluminium surface by a factor of 20, while Teflon provided a reduction of seven times [25].

Polyvinylidene fluoride (PVDF) coating was applied on to wind turbine blades made of glass fibre composite material to enhance ice phobicity. To create the roughened structure shown in Fig. 9, $NH_4HCO_3$ was added to the PVDF solution [43]. The pore sizes ranged from 1 to 5 µm, and a water contact angle of 156° and a water sliding angle of 2° were reported. Although an ice adhesion test was not conducted, an ice accretion test carried out at −10 °C with a water sprinkler (1 mm dia. water droplet size) spraying supercooled water onto horizontally placed samples, showed that there was negligible ice accretion within 50 min on the coated sample, while the bare sample collected about 40 g of ice. PVDF can also be combined with nano particles (epoxy siloxane mod ified $SiO_2$ [44], fumed silica [45], or graphene [46]) to create a porous structure and potentially increase the durability of polymer coatings.

In a separate study, a plasma enhanced chemical vapour deposition (PECVD) process was used to deposit a Si doped film (200 nm) followed by the application of a fluorinated carbon coating (10 nm) on smooth and roughened aluminium (Al 2024) surfaces. Ice adhesion and water contact angle measurements showed that the coating could reduce the ice adhesion strength on smooth and roughened Al 2024 by a factor of two; and the water contact angle increased by nearly four times on the rough surface [47]. A coating made of fluorinated acrylate

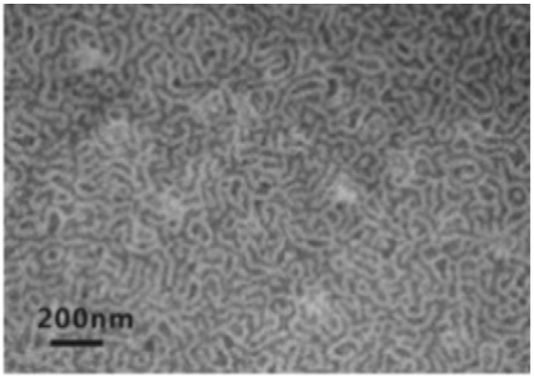


**Fig. 10.** Image illustrating the textured surface of the fluorinated polydimethylsiloxane. Reproduced from Ref. [48] with permission from Elsevier.

(polydimethylsiloxane b Poly) showed decreased ice adhesion (300 kPa) and extended ice crystallization delay (about 3 min at −15 °C) [48,49]. The nano scaled roughness of the surface can be seen in Fig. 10. Amphiphilic crosslinked hyperbranched fluoropolymers could lower the freezing point of water [50]. However, water molecules must be bonded to the surface in order for the coating to be effective, as molecular contact is required.

Fluoropolymer coatings impregnated with oxide and metal particles have drawn interest in the research community due to the ability to modify surface topology. Oxide and metal particles, such as $ZrO_2$, Ag, and $CeO_2$, were mixed with Zonyl 8740 (a perfluoroalkyl methacrylic copolymer) [31,51] to create the various coatings. The resulted surface morphology of different coatings is shown in Fig. 11. Ice adhesion tests

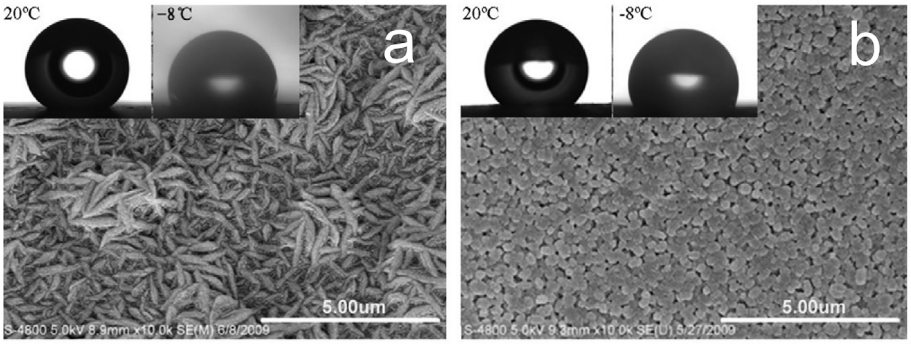


**Fig. 8.** Sintered PTFE coatings with gaps between the powder particles, imparting surface roughness. Figures reproduced from Ref. [42] with permission from Elsevier.

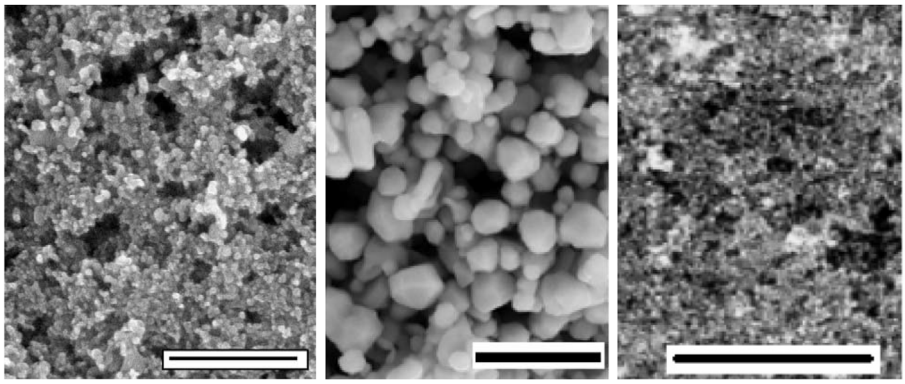


**Fig. 11.** Zonyl fluoropolymer coatings with various surface topologies created by the incorporations of particulates. Figures reproduced from Refs. [31,51] respectively, with permission from Elsevier.

were carried out by spraying supercooled water droplets (−10 °C, 2.5 g/m$^3$ LWC, 10 m/s wind speed and ~80 μm water droplet size) to generate glaze ice. When tested using a centrifuge ice adhesion testing apparatus, the results showed that ice adhesion was reduced up to 5.7 times on a nano Ag modified surface [51], compared to the uncoated surface. However, as later found by the same research group, the coatings deteriorated quickly after several icing and de icing cycles as was exemplified by the increased bonding strength to ice (Fig. 12). This was attributed to surface roughness changes after cycling. The results from several of these studies further stress the importance that a coating's durability is vital, particularly under repeated icing and de icing conditions.

The examples provided here suggest that this class of materials can provide both superhydrophobic and icephobic capabilities. However, the durability of these coatings requires further improvement.

### 3.3.2. Polysiloxane based viscoelastic coatings

This class of polymer coatings is based on viscoelastic, low Tg silicones. Silicones are polymers made of repeating units of siloxane along with functional constituents such as methyl, phenyl or trifluoropropyl. The low surface energy of the functional group bonds to the siloxane chain in combination with the low elastic modulus enables them to be icephobic [39].

From the perspective of reducing the adhesion of water to the solid surface, many researchers propose that a high contact angle in combination with a low sliding angle offer a reduction in water/ice adhesion to the surface [33,52]. As the bonding strength/energy between hydrogen atoms and fluorine atoms is three times greater than that of hydrogen atoms with dimethylsiloxane (or hydrocarbons) [33], many of the water/ice repellent coatings have been developed to make use of viscoelastic dimethylsiloxane polymeric materials. Indeed, viscoelastic coatings based on polydimethylsiloxane exhibited great ice adhesion reduction, near 100 times than that on a bare aluminium substrate [25]. The reduced ice adhesion was attributed to both the low surface energy and superior elasticity (perhaps to encourage interfacial sliding). This research also found that several existing so called “icephobic” wind turbine coatings had equivalent ice adhesion as that on bare aluminium surfaces. A plasma spray process was used to generate coatings from a liquid hexamethyldisiloxane feedstock (HMDSO, 98% purity, Aldrich) [53]. When applied onto an anodized aluminium surface, the coating could achieve an ARF of approximately four (from 400 to 100 kPa).

There are though several disadvantages associated with these types of viscoelastic elastomer coatings; their bonding strength to non silica/glass substrates is poor, needing a primer as an interface [54], and the environmental resistance to dust, sand, and ice particles is inferior to other coatings. Additives can be incorporated to render it more wear and erosion resistant, while at the same time imparting surface roughness changes and superhydrophobicity. A coating manufactured using a mixture of tetraethyl orthosilicate and n octyltriethoxysilane with the addition of silica nanoparticles (functionalized with octyl triethoxysilane) yielded a contact angle 153° [55]. Poly dimethylsiloxane (PDMS) coatings with the incorporation of nano silica were developed to reduce ice accumulation on power line insulations [56]. Coatings were deposited using a sprayed gel process, with the resulting coating morphology shown in Fig. 13.

PDMS coatings with nano silica particles of less than 100 nm in diameter were observed to exhibit superior ability in shedding water droplets, instead of allowing droplets to freeze upon impacting the surface [57], due to a high water contact angle of near 161° along with a low water roll off angle. The rate of ice accumulation was also reduced as a result. Under a supercooled water droplet spray condition, test samples held at −5 °C had negligible ice deposition for up to 0.5 h. The improved icephobic properties were attributed to both hydrophobicity and reduced ice adhesion to the coating. Similarly, other researchers also investigated the hydrophobic properties of PDMS with silica and PDMS with silica and metal oxides ($Al_2O_3$, $Cr_2O_3$, etc.) [58]. The addition of metal oxide was reported to impart a catalytic function to the reaction between the $SiO_2$ particles and polymer. Other researchers developed transparent superhydrophobic coatings combining ZnO and $SiO_2$ with methylphenyl silicone binder [59]. An “erosion and icephobic fluorosilicone coating” was marketed by AMES Shied [60]. Presumably, the erosion resistance is provided by the incorporation of particulates. Lastly, when using a composite coating structure with nano particles, it must be realized that the particle sizes for

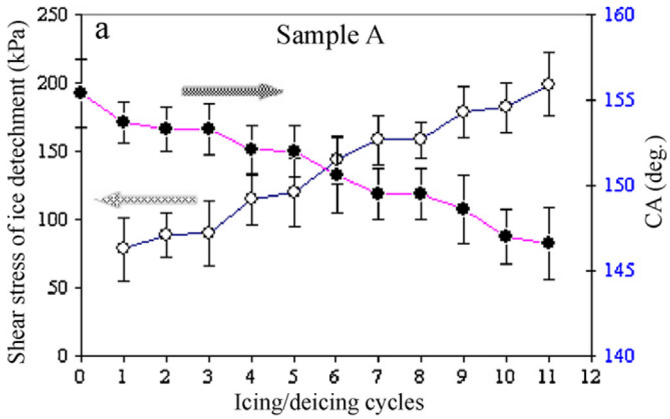


**Fig. 12.** Increase in coating-ice adhesion with each icing/de-icing cycle (the microstructure of sample A is shown in Fig. 11 (c). Figure reproduced from Ref. [31]) with permission from Elsevier.

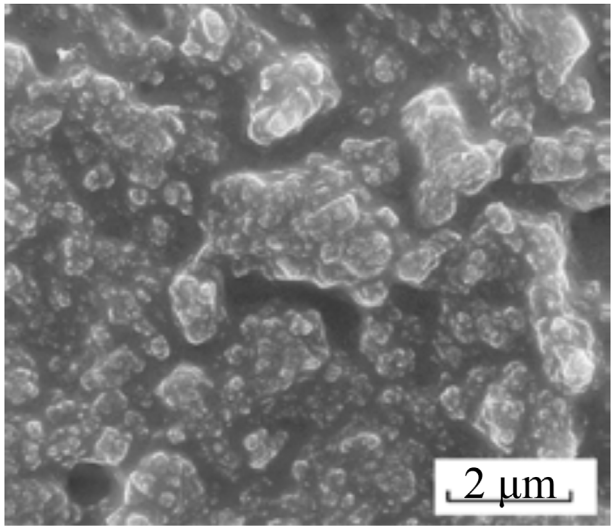


**Fig. 13.** PDMS modified nano-silica hybrid coating that exhibits superior ice accumulation resistance. Reproduced from Ref. [56] with permission from Taylor & Francis.

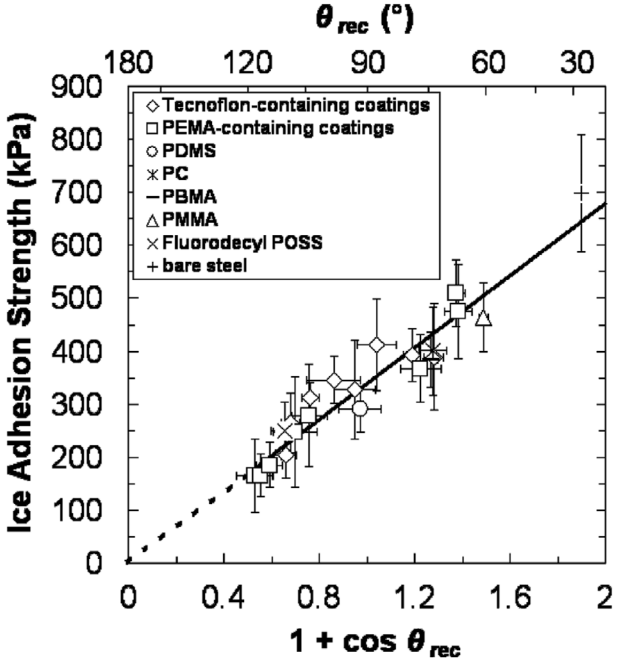


**Fig. 14.** Relationship between ice adhesion and receding contact angle where $(1+\cos\theta_{rec})$ is proportional to the practical work of adhesion. Figure reproduced from Ref. [32] with permission from American Chemical Society.

superhydrophobic and icephobic coatings are in a different dimensional scale [57]. The selection of additives must be tailored for intended applications.

The long term stability of siloxane based icephobic coatings has not been well established. The plasma sprayed hexamethyldisiloxane reported in Ref. [53] showed surface degradation after 15 cycles of icing/de icing. Aluminium samples coated with perfluoro octyltriethoxysilane also experienced degradation in terms of its ice adhesion increase and water repellency reduction [31]. The same study also found that "wet" samples, exposed to a condensation condition prior to an icing test, produced ice adhesion strength values as large as three times that of dry samples. Similarly, ice adhesion to coatings made of perfluorodecyltriethoxysilane (FAS 17) or stearic acid (SA) increased about four times after 20 cycles of icing and de icing [24]. Hydrolysis was considered as a probable reason when the coating was in contact with water or ice for long period of time. In another study, although limited hydrolysis of the siloxane bonds was observed, the contact angle and roll off angle were not significantly influenced after 100 cycles during a 250 h test [61].

### 3.3.3. Metallic coatings

Erosion from rain, sand, and dust particles is a critical issue for aerospace surfaces, thus coatings should have sufficient erosion resistance to survive in the operating environment. Metallic coatings have become of interest, with some possessing icephobicity [62,63]. Titanium based coatings are of particular interest with work done on titanium nitride (TiN), titanium aluminium nitride (TiAlN), and commercially pure titanium. In a study conducted by Palacios et al., TiAlN increased the erosion resistance of the leading edge erosion shield of a helicopter by two orders of magnitude [63]. The TiN samples also improved the erosion resistance, however, they increased the ice adhesion strength when a performance metric that normalized the adhesion strength as a function of the roughness was introduced. The TiAlN samples had a lower ice adhesion strength than the titanium substrate when the roughness was below 0.6 μm [64]. Although the roughness of the surface increases with usage, polishing the surface prior to initial commissioning will minimize the initial roughness and maximize the overall performance.

A study by Jung et al. tested a variety of icephobic, hydrophobic, and hydrophilic coatings and found that the hydrophilic diamond coatings yielded the greatest freezing delay time [65]. Although these surfaces are hydrophilic, their very low surface roughness (1.4 6 nm) is near the critical ice nucleation radius, thus significantly delaying the freezing time. The critical ice nucleation radius is the critical size that an ice crystal must reach for freezing to occur. This low surface roughness ensures that ice cannot form within the asperities, leading to a low ice adhesion strength.

### 3.3.4. Surface texturing and topology modifications

One study found that the ice adhesion to known, flat surfaces may have reached a physical limit [6]. This was observed from a large test matrix of samples, including 21 different materials with different water contact angles. As shown in Fig. 14, the ice adhesion strength decreases as the receding contact angle increases. However, as no known material has a receding angle greater than 120° [6], it was suggested that any further reduction to ice adhesion beyond 150 kPa must be achieved by surface topology changes or polymer molecular engineering [39]. Based on observations of reduced ice adhesion with increased water contact angles, roughened surfaces that allow the entrapment of air within their asperities have been proposed as means to reduce ice adhesion. However, these structures, which are difficult and costly to manufacture, are prone to damage during cyclic icing and de icing processes as the nanofeatures may break off [24,66]. Furthermore, when the atmospheric humidity level is high, the nature of the roughened/textured surface can switch from a Cassie Baxter state with trapped air below the water droplet to a Wenzel state [19,67] of low water contact angles (< 90°). The following sections summarize several of these textured coatings/surfaces with enhanced icephobicity, along their application methods.

*3.3.4.1. Textured anodic aluminium surface.* Aluminium alloys are commonly used to manufacture aircraft structural components. Even with the wide spread use of composite materials and fibre metal laminates, aluminium will remain a common substrate material to manufacturing aircraft. To prevent corrosion or accept paints, aluminium alloys are routinely anodized and primed. The existing anodizing processes, whether by sulphuric (SAA), phosphoric (PAA), or oxalic acid, may be coupled with anti icing features. Both SAA and PAA could generate a control pitched surface profile and render the surface hydrophobic after post processing with HDFS (Heptadecafluoro 1,1,2,2

tetrahydrodecyl trichlorosilane) [68]. Examples of these nano surface structures are shown in Fig. 15. The resulting contact angle changes from untreated states were significant, as shown in Fig. 16. Post anodizing processing with FOTS (fluorooctyltrichlorosilane) hexane treatment can render the anodized surface superhydrophobic, as the reported contact angles were greater than 150° [69].

However, when utilizing surface texture for anti icing purposes, it must be employed judiciously as a groove with a characteristic width ranging from 0.1 nm to 2 nm may promote ice crystal nucleation [70].

*3.3.4.2. Laser texturing.* A laser has the potential to micromachine any surface. With the wide spread use of lasers in processing and potentially in additive manufacturing, the use of laser profiling to create icephobic surfaces is appealing from the perspective of manufacturability and durability. One study showed that laser texturing had the ability to impart icephobicity to both metal substrates and diamond like carbon (DLC) coatings [71]. The surface morphology of the DLC coating is shown in Fig. 17.

Laser texturing was also used to create a hydrophobic titanium (Ti) surface. Here a pulsed ultrafast laser micro texturing process was em ployed as shown in Fig. 18 (a) and the result was a Ti surface with pillars several microns in height (Fig. 18 (b)) [72]. After laser proces sing, a thin fluoropolymer coating was applied to achieve a contact angle of 165° and a sliding contact angle of < 7°. Linear abrasive wear test results indicated that the laser processed surface can maintain a contact angle > 150° after three abrasion cycles using a 350 g mass (108 kPa applied pressure). Some superficial wear occurred due to the fracture of the upper 10% of the pillars, again illustrating the im portance of suitable mechanical durability for harsh application con ditions.

*3.3.4.3. Two tiered surface structuring.* A polymer, whether it is flat or contoured, can be implanted with particles to create bimodal surfaces containing micro and nano structure. Illustrated here are two of such structures; one engineered with two sizes of silica particles (10 nm and 50 nm) and the other with lithography followed by spraying 10 nm silica particles dispersed in epoxy, as shown in Fig. 19 (a) and (b), respectively. Epoxy is used in many aircraft composite systems; the attachment of surface features into the epoxy matrix has the potential to be part of the composite manufacturing process. Micro and nano sized silica in an epoxy matrix provided hydrophobicity, while at the same time improving wear resistance [73]. The resulting hierarchical surface structures (Fig. 19) with bimodal features render the surface capable of de icing, self cleaning and anti fouling. However, it is not clear if this coating structure can sustain anti icing characteristics under a high humidity environment as the increased surface area, once covered by frost, may result in increased ice adhesion. In addition, the resistance to abrasive wear is not known.

In another study, a micro scaled surface was created first with a wet etching process to generate cones about 60 μm apart; the surface was

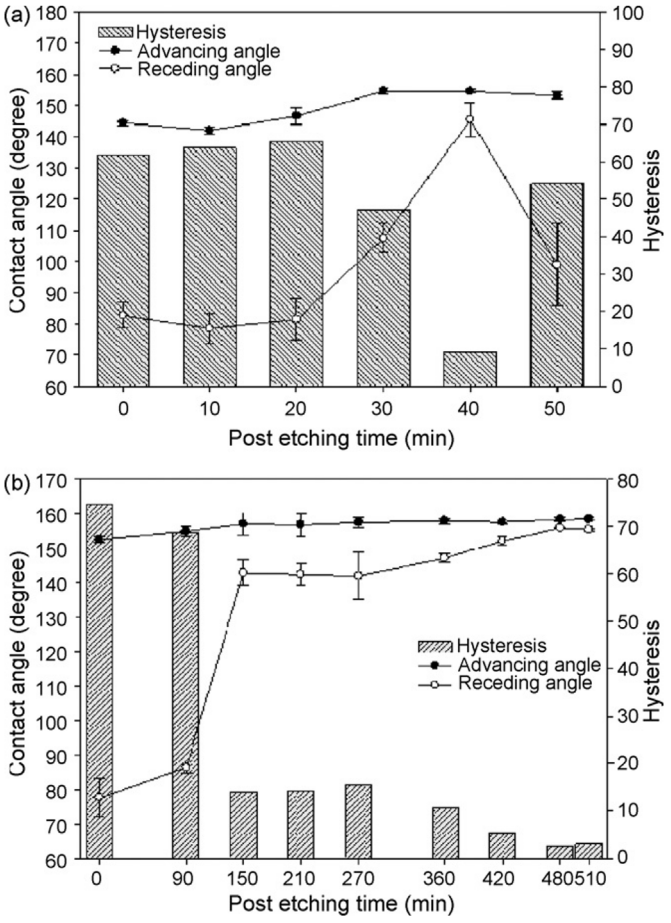


**Fig. 16.** Contact angle and hysteresis changes. (a) HDFS treated SAA and (b) HDFS treated PAA. Figures reproduced from Ref. [68] with permission from Elsevier.

then etched with deep reactive ion etching (DRIE) to grow "grass" on the entire surface, as show in Fig. 20. Finally, the profiled surface was coated with perfluorooctyl trichlorosilane (in hexane solution). The resulting surface was tested under 65% relative humidity (at an am bient temperature of 22 °C) with samples cooled to a temperature of −10 °C using a cooling stage [74]. Based on a detailed in situ frost formation observation, it was concluded that the engineered structure was able to retard the frost formation process through a higher energy barrier for droplet coalescence and nucleation.

A similar structure containing micro meter pillars (fabricated with photolithography and cryogenic ICP etching) with nano scaled surface roughness (PECVD $SiO_2$ followed by ICP etching) and a final layer of

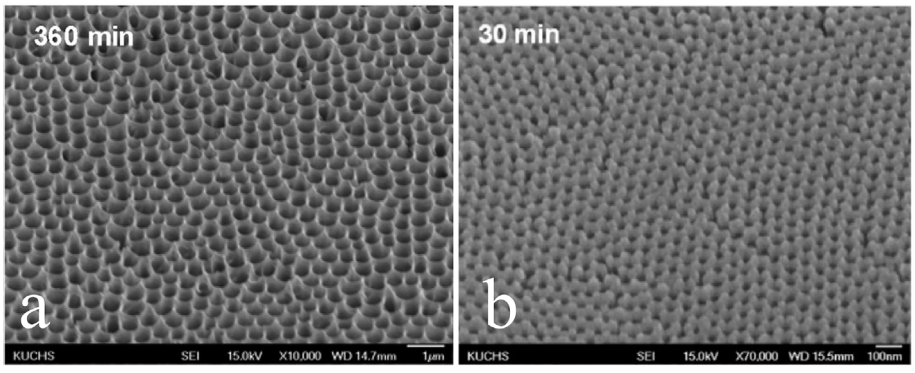


**Fig. 15.** SEM images of (a) PAA (360 min of etching) and (b) SAA surface (30 min of etching). Figures reproduced from Ref. [68] with permission from Elsevier.

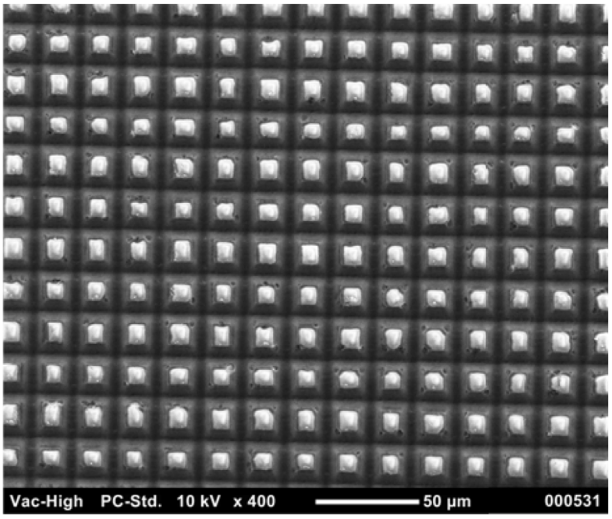


**Fig. 17.** SEM image of laser profiled DLC. Reproduced from Ref. [71] with permission from Elsevier.

perfluorodecyltrichlorosilane (FETS) [75] has shown that the freezing delay of a sessile supercooled water droplet at −21 °C is up to 25 h. The authors attributed this long nucleation delay (longest based on litera ture) to the presence of an interfacial quasi liquid layer.

Despite the exceptional anti icing and hydrophobic properties of these highly engineered surfaces, one must be aware of the effect of surface roughness under various icing conditions. Certain roughened surfaces can accelerate the heterogeneous nucleation of ice while others may increase the ice adhesion strength. A review written by Schutzius et al. revealed that for a multi tier surface structure, each roughness scale must address a specific target; the micro scale has a low adhesion strength while the nano scale texture resists droplet impingement and promotes rebound [76]. Additionally, the processes used to create these surfaces, such as photolithography, CVD, PVD, etc., are costly and not suitable for mass production or on large structures.

*3.3.4.4. Textured and coated stainless steels.* Stainless steels are used to house many aircraft instruments and gauges; anti icing ability is also beneficial for many applications. Here a simple chemical etching (50% $FeCl_3$ solution) followed by the deposition of a layer of nano silica dispersed in methoxy silane has rendered a stainless steel icephobic, based on qualitative outdoor snow and freezing rain test [61]. In particular, the treated surface was able to sustain a water contact angle of 155° after 100 icing/de icing cycles and a cavitation erosion simulation test.

*3.3.5. Liquid filled porous surfaces*

*3.3.5.1. Slippery Liquid Infused Porous Surfaces (SLIPS).* Inspired by plants and insects in nature, a class of Slippery Liquid Infused Porous Surfaces (SLIPS) has been created by several researchers [34,77,78]. To overcome the deficiency of hydrophobic surfaces in a moisture saturated environment (due to frost formation), a new composite surface design was created to minimize the frost formation on the surface. In this design, shown in Fig. 21, a nano porous polymer structure was first fabricated using electrodeposition; it was then followed by the infiltration of a low freezing point fluorinated liquid. The liquid is retained on the surface by the nano structure, giving the surface a “slippery” nature [34]. In fact, a pitcher plant has a similar slippery liquid filled porous structure. Both of which rely on the simple fact that the smoothest surface is a liquid. This engineered composite structure has a combination of low contact angle hysteresis (for water droplets to roll off the surface) and low ice adhesion of 16 kPa [41]. Despite the superior icephobic properties, lubricant depletion would occur and compromise the performance.

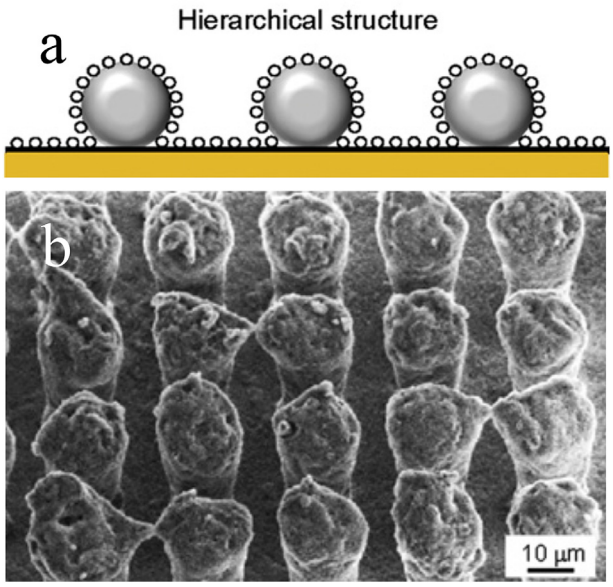


**Fig. 19.** Bimodal surface structures consisting of (a) two powder particle sizes and (b) surface structure created with lithography and spraying of nano-sized silica. Figures reproduced from Ref. [73] with permission from Elsevier.

*3.3.5.2. A lubricant infused electrospray silicone rubber anti icing coating.* In this study, a heptadecafluorodecyltrimethoxysilane fluorinated coating was fabricated to exhibit a hierarchically porous structure [79]. This structure was designed with the objective to improve upon the existing SLIPS [34] so that ice nucleation can be delayed for a longer duration and the period prior to lubricant depletion extended. The porous structure was infiltrated with a perfluoropolyether lubricant. The results showed that the ice

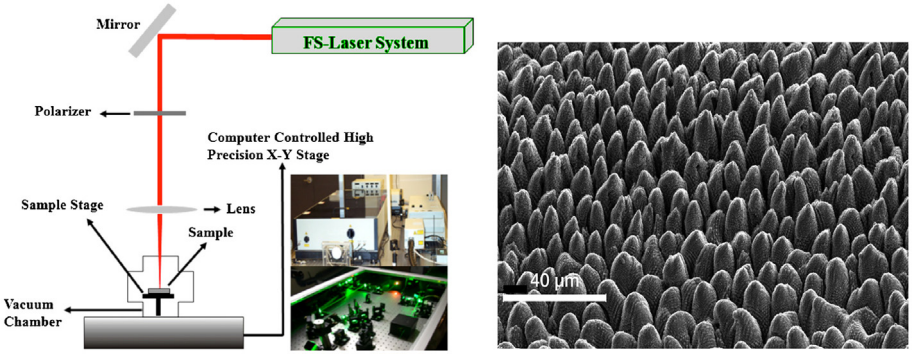


**Fig. 18.** Laser micro-texturing process (a) and the resulted surface morphology (b). Figures reproduced from Ref. [72] with permission from IOP Science.

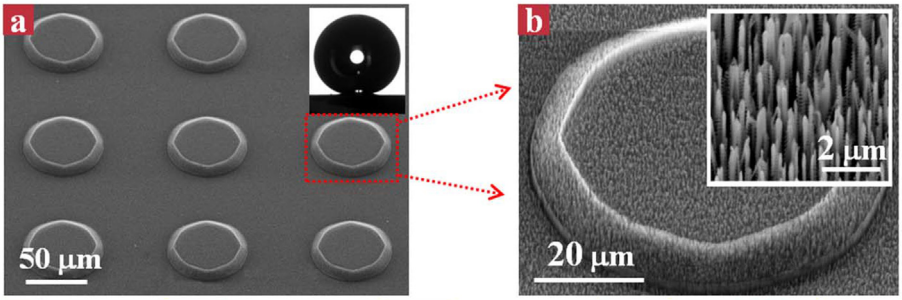


**Fig. 20.** SEM images of a two-tiered surface structure. The diameter of the "grass" is about 300 nm. Figures amended and reproduced from Ref. [74], published under a Creative Commons Attribution 3.0 Unported License.

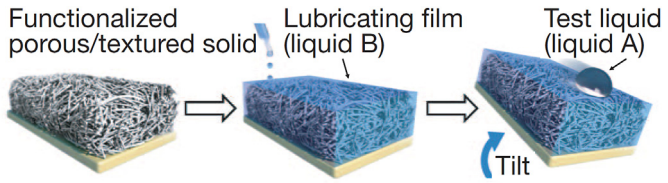


**Fig. 21.** Illustration of the SLIPS structure in which liquid infiltrated into a porous surface layer, enabling the solid surface to be perfectly flat and saturated with liquid. Reproduced from Ref. [34] with permission from Springer Nature.

adhesion strength can be reduced to 60 kPa (vs 1400 kPa for the uncoated substrate). However, this value increased to 600 kPa after 20 cycles of frosting and defrosting (the frosting process was carried out at −14 °C in an environment with 80 90% humidity; after the surface was covered with frost the temperature was raised to room temperature and then the cycle repeated). The degradation was due to the loss of lubricant with each cycle. Based on a similar principle, others showed a silicone oil infused polydimethylsiloxane coating achieved a low ice adhesion of 50 kPa (3% of that of bare aluminium) [80]. Similarly, in another study of an oil infused porous PDMS coating, the ice adhesion strength was reduced to 38 kPa, about 50% the ice adhesion strength of a smooth PDMS surface and ~30% of micro featured PDMS surface shown in Fig. 22 [81].

*3.3.5.3. Antifreeze releasing coatings.* A bioinspired coating was reported in Ref. [82] where a porous superhydrophobic layer with wicking channels was embedded. These channels were then infiltrated with antifreeze agent. Tests in frosting, simulated freezing fog, and freezing rain showed that the onset of either frost, rime or glaze ice formation was delayed for at least 10 times longer than that of other coating systems, including the lubricant filled surfaces. Depending upon how easily the antifreeze agent can be replenished during service, it has a potential aircraft application since the antifreeze agent is regularly applied to aircraft in icing conditions before taking off.

The latest, commercially available room temperature vulcanizing (RTV) R 1009 (*Nusil Sol Gel Vulcanized Silicone Coating*) has seen an ice adhesion five times less than the previously marked anti icing coating R 2180 [83], also developed by the company [84]. The comparison of NuSil R 2180 with other commercial coatings is illustrated in Fig. 23. Although not being disclosed in public, it was speculated that this series of vulcanized coatings contains a slow releasing agent of freezing point depressant [6]. The authors of this paper are currently investigating the use of silicone R 1009 in conjunction with piezoelectric actuators in a hybrid coating/ultrasonic de icing system.

Among all types of anti icing coatings described in this section, the lowest ice adhesion was reported among the SLIPS category of coatings [39]; at 16 kPa, the ice adhesion on these surfaces is nearly two orders of magnitude lower than that on uncoated aluminium surfaces. In terms of the durability of these coatings, as the liquid (lubricant, oil or anti freezing agent) is held in place via weak capillary force, its depletion or dilution, particularly during repeated icing/de icing, is likely to occur, thus rendering the coatings non functional if an active charging system is not put in place [15].

*3.3.6. Icephobic polymer coatings designed based on cross link density and interfacial lubricant*

The newest and perhaps the most advanced icephobic coating series were designed to enable polymer chain mobility within an elastomer matrix, hence creating a slip boundary condition between the ice and coating surface [39]. As the shear stress to cause slip at the interface is governed by $\tau = Gfa/kT$ (where $G$ is the physical stiffness or shear modulus under isotropic conditions, $f$ is the force needed to detach a single chain with $a$ length, $k$ is the Boltzmann's constant, and $T$ is the temperature) and the polymer cross link density $\rho^{CL}$. The authors pro posed two methods to reduce the adhesion of ice on a polymer surface by (1) using a polymer with low cross link density and (2) the addition of miscible lubricant to enable interfacial slippage. Using the first method, a low cross link density PDMS was able to arrive at a low shear strength of 33 kPa, without the addition of lubricants nor the presence of texture/roughness. With the addition of interfacial lubricants (such as silicone, krytox or oil) into the polymer structure chemically (vs. physical infiltration in SLIPS), the adhesion strength was further re duced to 6 kPa. Other polymer systems (polyurethane (PU), fluorinated polyurethane (FPU), and PFPE, shown in Fig. 24) also exhibited similar improvements with cross link density reduction, although the addition of an interfacial lubricant had a greater impact on the ice adhesion reduction. Furthermore, when these engineered icephobic coatings were subjected to repeated icing/de icing cycles, wear, and outdoor weathering, they consistently demonstrated superior durability to commercially available (Nusil, NeverWet) and SLIPS coatings.

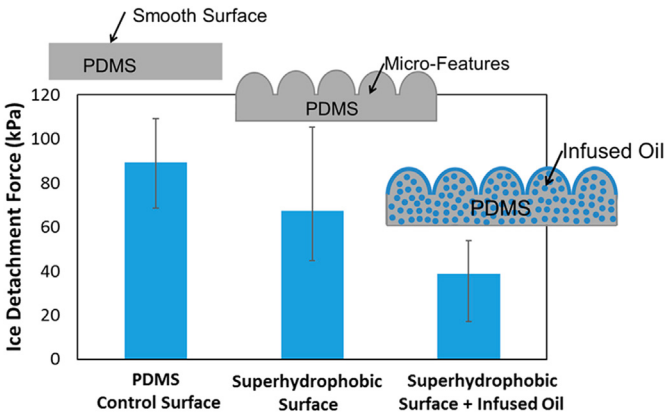


**Fig. 22.** Slippery liquid-infused porous surfaces (SLIPS) with an optimal combination of high water repellency and icephobicity. Reproduced from Ref. [81] with permission from American Chemical Society.

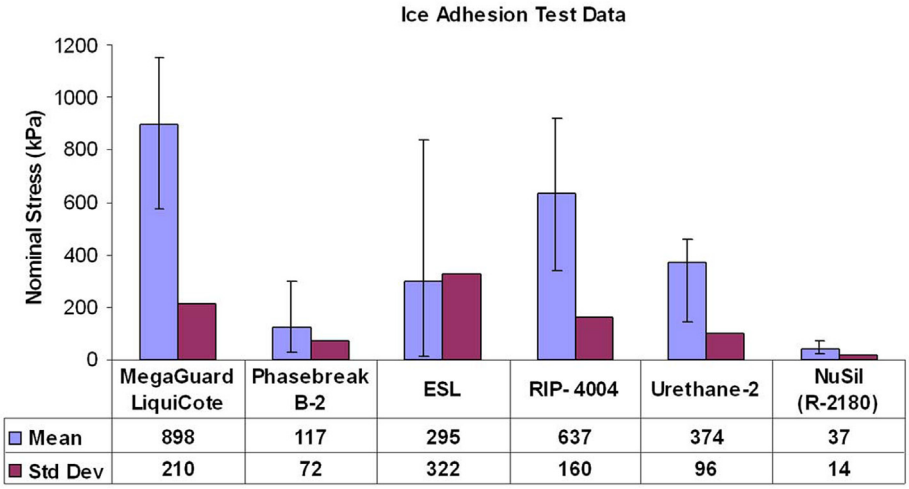


**Fig. 23.** Laboratory ice adhesion test results of R-2180 and several other commercial icephobic coatings. Reproduced from Ref. [128] with permission from CRREL.

*3.3.7. Carbon nanotube and graphene containing coatings*

In terms of durability and electrical properties required for potential aircraft applications, carbon nanotube (CNT) and graphene may pro vide the needed physical/mechanical properties, and offer a practical way to modify the surface topology and impart hydrophobicity and perhaps icephobicity. Although not being tested for anti icing, a CNT forest structure was fabricated with vertically aligned nanotubes (CNTs) within a PTFE matrix [85]. A micrometre scaled water droplet was completely suspended on top of this surface as shown in Fig. 25. In another study, a composite epoxy resin, impregnated with CNTs, was sprayed onto a substrate and superhydrophobicity was reported [86]. The use of nanotubes in a coating provides an opportunity to in corporate heating into the surface for de icing and anti icing purposes. In fact, resistance heating was enabled in a film of graphene nanoribbon (with large aspect ratio to form electrical pathway) within an epoxy matrix [87].

Unlike that discussed in the preceding sections where coatings were intended to provide reduced ice adhesion and delayed freezing of su percooled water droplets, one coating developed for protecting aircraft radomes was based on an active mechanism where current is passed through the layer to generate heat for de icing [88]. In this research, graphene nanoribbons (GNRs) coating (100 nm), which is transparent to radio frequencies, was applied to substrate using an airbrush at 220 °C. A de icing test was carried out at −20 °C and successful ice removal was reported. In another report, a Carbo e Therm coating was applied on curved surfaces and it could be electrically heated for use in the non hazardous low voltage range (e.g. 12/24 V). It contains carbon nanotubes and graphite to render it electrically conductive [89]. By

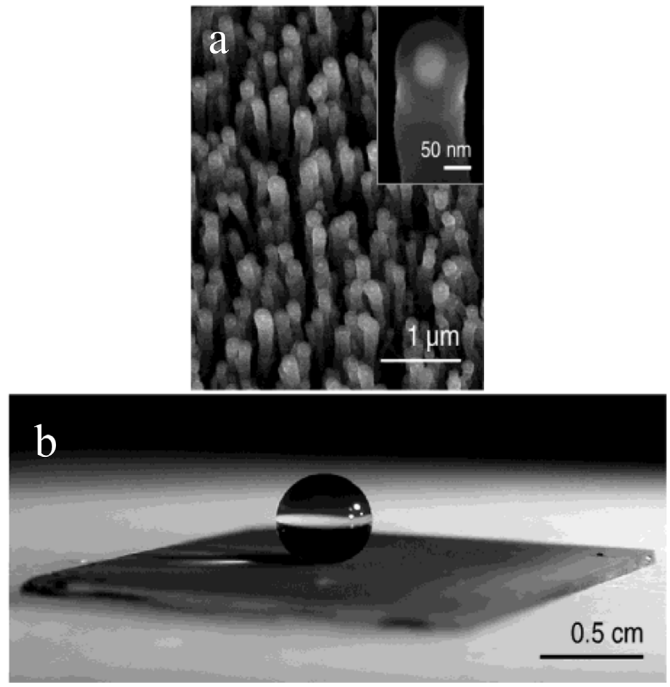


**Fig. 25.** (a) SEM image of a carbon nanotube forest coated with PTFE and (b) water droplet suspends on top of the surface. Figures reproduced from Ref. [85] with permission from American Chemical Society.

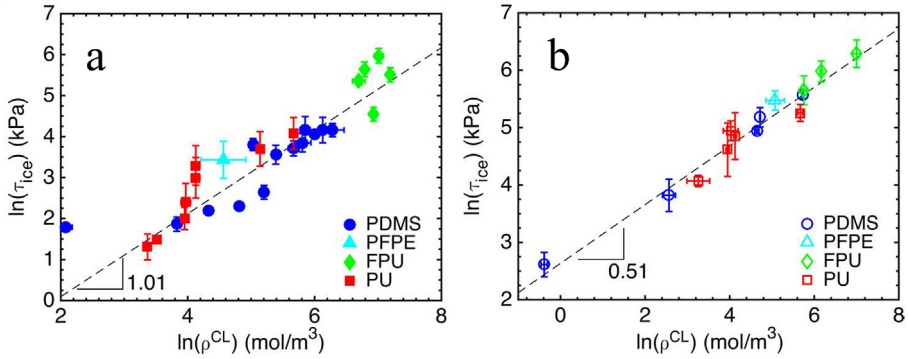


**Fig. 24.** Ice adhesion strength is demonstrated as a function of cross-link density, (a) With interfacial slippage and (b) without interfacial slippage. Figures reproduced from Ref. [39] with permission from AAAS.

combining icephobic coatings with conductive additives, the result is a coating with both passive and active anti icing and de icing cap abilities. Lastly, the approach used in SLIPS can be incorporated into these functional coatings; an example of which is a spray coated per fluorododecylated graphene nanoribbons with the addition of a lu bricating slippery surface [90].

#### 3.3.8. Other coating types

A negatively charged surface has been reported to have the function of reducing freezing temperature, in particular, a textured hydrophobic stainless with anionic polyelectrolytes brushes was found to reduce the freezing temperature by at least 7 °C than that measured on untreated surface [91]. Coating material with polarity changes (generated for example by an externally applied electric field during the coating process) also has the effect of reducing the freezing temperature of water on the surface by restricting heterogeneous ice nucleation [67]. Ultimately, if a coating can be developed to delay the freezing of su percooled water droplets to beyond −50 °C, icing may no longer pre sent an issue during high altitude flight.

Icephobicity can also be combined with other functions such as aircraft drag reduction. From the study of many living species, it has been realized that many surfaces have the natural ability to repel water (lotus leaf, pitcher plant, cicada, etc.) and also possess superior aero dynamic performance (butterfly wings and shark skin, as shown in Fig. 26) [92,93]. In fact, shark skin topology can help reduce drag by up to 8% and fuel consumption by 1.5%, not to mention that it possesses the needed surface topology for potential icephobic properties.

Also inspired by nature, another development in this area is the creation of biological antifreeze proteins. This is a new and different area that may see future development of synthetic macromolecules for preventing ice crystals from growing [94]. A detailed review can be found in the quoted reference.

## 4. Harmonization of tests for assessing the durability of functional icephobic coatings

The benefits expected from the use of icephobic coatings are to limit ice accretion on an aircraft surface during flight in icing conditions or to facilitate ice shedding on rotating components or components exposed to aerodynamic shear forces. When combined with an active IPS (heating elements, mechanical actuators, surface acoustic wave actua tors, piezoceramic actuators, etc.), the technology should reduce the energy consumption of the overall IPS.

To be applied onto aircraft, icephobic coatings must meet several major requirements including but not limited to, erosion resistance (rain, sand), chemical exposure tolerances, resistance to UV exposure and thermal shocks, remain operative in representative icing flight conditions (e.g., 25 FAR Apps. C, O, or P), comply with the latest REACH (Registration, Evaluation, Authorisation and Restriction of Chemicals) regulations [95], and be compatible with all existing air craft (engine/airframe/nacelle) surface finish requirements.

### 4.1. Preliminary tests on as manufactured icephobic coatings

#### 4.1.1. Contact angle, surface roughness, elasticity, coating thickness and FT IR analysis

To verify the properties of an icephobic coating, a series of tests must be performed to determine the wettability via water contact angle measurements, the surface roughness, the elasticity (when applicable, e.g. via nano indentation measurements), the thickness of the coating (e.g., via eddy current measurements), and a surface spectroscopic analysis (e.g., FT IR or surface Raman) for controlling surface chemistry and cleanliness of the samples.

#### 4.1.2. Ice adhesion strength, cross cut & REACH compliance

The ice adhesion strength must be determined using one of several methods currently used in several labs (e.g., tensile mode (Mode I), shear mode (Mode II), rotating arm, or bending test) in well defined, simulated atmospheric icing conditions in icing wind tunnel tests (IWTT). Since not all conditions can be tested, a design of experiments (DoE) approach can be employed for selecting a reduced number of icing parameters that are most representative of atmospheric icing, e.g. including a rime, a glaze, and two mixed icing conditions outlined in Table 3 [96,97].

Cross cut adhesion tests [98] of the coatings to the substrates can be performed according to the ISO 2409 procedure only on polymer coatings. The test is not applicable to icephobic functionalized metals or ceramic materials, which are used either bare or the coating applied (like, PFPE or perfluorinated silanes or siloxanes) is only a mono molecular thick polymer film and as such, its adhesion to the substrate is not detectable by the cross cut test.

REACH compliance must be assessed for all icephobic coatings ac cording to the regulation.

#### 4.1.3. Rain erosion testing

Rain erosion resistance must be tested according to well defined and accepted standards for aerospace applications, such as the P JET or the whirling arm tests which run according to the standard DEF STAN 00 35 [99]. A set of representative testing conditions is listed in Table 4.

The working principle of the P JET, developed at Airbus, is that a jet of water accelerated by a pump to a set velocity is chopped into short segments by a disc with two openings rotating at a set speed. The front heads of the water segments acquire a hemispherical shape due to surface tension and aerodynamic drag. The segments then impinge on the surface of the test coupon that can be tilted at a desired angle of incidence. The number of impact events at the same location can be varied depending on the need and the type of coating: for our purposes, the number of impacts was varied between 20 and 3000. The testing schematic is shown in Fig. 27 while results of the droplet impact on several surfaces is shown in Fig. 28.

#### 4.1.4. Sand erosion testing

Sand erosion resistance must be tested according to well defined and

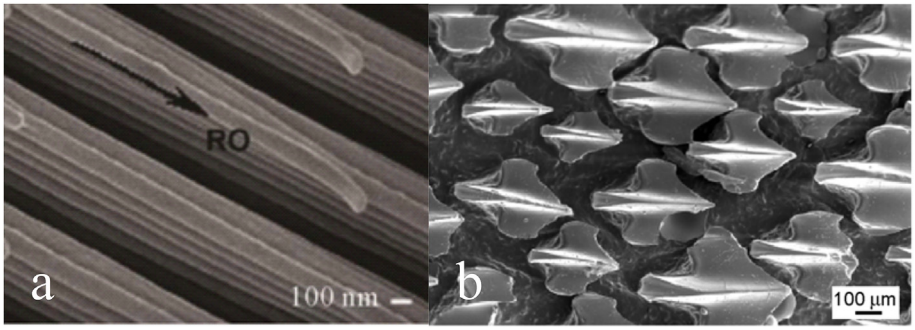


**Fig. 26.** (a) Butterfly wing and (b) shark skin. Figures reproduced from Refs. [93,129], with permission from RSC and IOP Science respectively.

**Table 3**
Reduced set of four representative icing conditions that can be selected for ice adhesion tests.

| Ice type | Total air temperature (TAT) [°C] | Airspeed [m/s] | Liquid water content (LWC) [g/cm$^3$] | Mean effective droplet diameter (MVD) [μm] |
|---|---|---|---|---|
| Rime | 20 | 50 | 0.3 | 20 |
| Mixed/rime | 5 | 50 | 0.3 | 20 |
| Mixed/glaze | 20 | 50 | 0.8 | 20 |
| Glaze | 5 | 50 | 1.0 | 20 |

**Table 4**
Example of DEF STAN 00-35 rain erosion testing parameters used with P-JET.

| | |
|---|---|
| Velocity (m/s) | 225 |
| Drop size (mm) | 2 |
| Disc rotational frequency (Hz) | 20 |
| Nozzle diameter (mm) | 0.8 |
| Sample-to-nozzle distance (mm) | 60 |
| Impact angle (°) | 90 |
| Test sequence (no. of drops) | 20 → 50 → 100 → 250 → 500 → 1000 → 2000 → 3000 |

accepted standards for aerospace applications, such as ASTM standard G76 04 [100] which is used for the Plint TE 68 Gas Jet Erosion Rig. A set of representative parameters for this test is listed in Table 5.

The working principle is that a defined mass of sand particles is suspended in the flow of a carrier gas and accelerated towards a nozzle that directs the mixed stream of gas and particles towards the sample surface as outlined in Fig. 29. After having eroded the sample with a defined mass of sand (erodent), the weight loss of the sample is determined (eroded mass), and the test continues. The test is stopped when the maximum mass of erodent has been applied or when the coating is fully eroded and the primer or the substrate become exposed.

During the sand erosion test, different surfaces will exhibit different behaviours. For example, elastomers undergo slow deformation while the sand particles accumulate and will suddenly fail, rendering the coating useless. On the other hand, polymers erode linearly with increasing erodent mass while functionalized metallic surfaces typically show no visible damage until the metal itself is eroded.

### 4.2. Functional performance of icephobic coatings

After having discussed how to assess the basic properties of icephobic coatings, we want to introduce an example of how to assess the functional performance of icephobic coatings. Functional performance testing investigates how the icephobic properties of the coatings deteriorate during (simulated) operation. This analysis goes one step beyond that of the previous section that investigated the durability of the coatings themselves; here it is intended to assess the durability of the icephobic property.

#### 4.2.1. Preliminary considerations

The first consideration to be made is that there is, so far, no established standard known to us for testing the functional durability of icephobic coatings, meaning the durability of the coating itself and the durability of its functionality in relevant (simulated) environmental conditions. One thus needs to define a new set of tests and measurables that allow for a meaningful and reliable assessment. The following solutions could offer viable alternatives:

- **Solution 1**: Expose all samples to sequential degradation tests (erosion, UV, thermal, fluids, etc.) and after each step determine the ice adhesion strength in an IWTT
- **Solution 2**: Simulate accelerated degradation (erosion, UV, thermal, fluids, etc.) over the whole sample area and perform wettability tests only (contact angles of water drops) on the degraded coatings, taking the degradation of surface wettability as a strong indicator for adhesion strength to ice

Solution 1 is very expensive and time consuming while solution 2 is less costly and time consuming, but might provide only an incomplete set of results. Therefore, there is a strong need of defining a more rapid, but complete screening standard for functional tests in the future.

#### 4.2.2. Simulation of mechanical degradation

For the mechanical degradation simulations, a sandblasting test can be used to simulate erosion and a measurement protocol can be developed. The discrete time steps of sandblasting by which the thickness of the coating is gradually reduced would need to be standardized. These time steps depend on the specific material of the coating and must be found empirically. After each time step, the CA and the RoA of water drops on the surface must be determined.

We must point out here that, since there are no existing ISO guidelines or standards to follow for such a characterization, the measurement protocol must be set up and the sandblasting parameters chosen according to a best practice that must be developed during the course of the testing.

#### 4.2.3. Simulation of physical chemical degradation

For simulating chemical degradation and stability, one must perform Q UV tests, immersion in at least two reference fluids, e.g. Skydrol

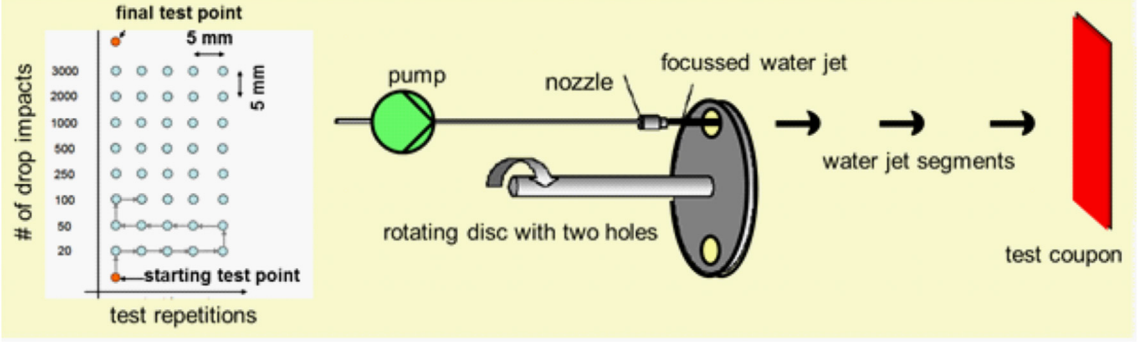


**Fig. 27.** (left) Testing program showing the array of drops impacting a test coupon; (right) working principle of the rain erosion test rig P-JET: a continuous water jet is cut into short segments by a rotating mechanical chopper disc.

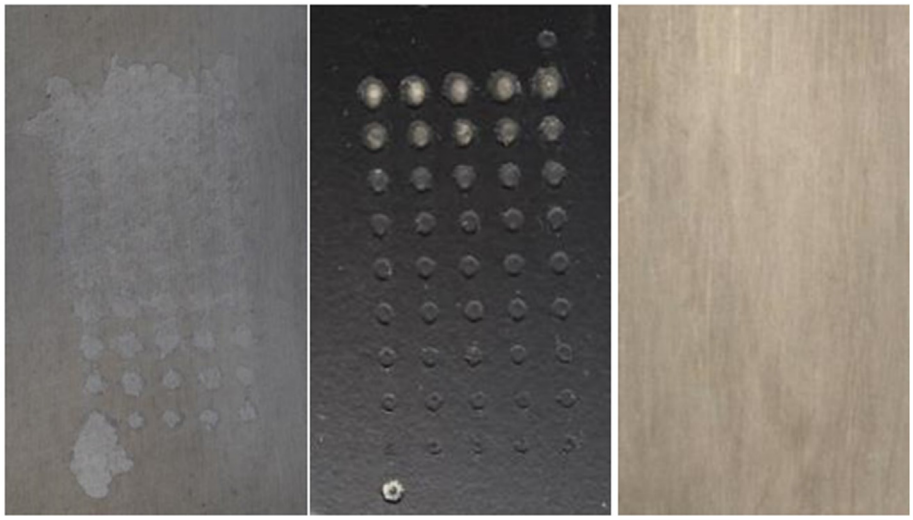

**Fig. 28.** Rain erosion results for three coupons. From left to right: an elastomer coating showing heavy delamination, polyurethane coating showing local damage increasing with number of drop impacts, and a functionalized metallic surface showing no visible damage.

**Table 5**
Example of ASTM G76 sand erosion testing parameters.

| | |
|---|---|
| Velocity (m/s) | 50–65 (270 mbar pressure at nozzle) |
| Particle size (μm) | 250–270 (nearly spherical silica particles) |
| Discharge rate (g/min) | 2 |
| Sample-to-nozzle distance (mm) | 20 |
| Impact angle (°) | 20 |
| Test sequence (g) | 0 → 5 → 10 → 20 → 50 → 100 → 150 → 200 |

(hydraulic fluid) and Kilfrost (de icing fluid), and a thermal treatment. The Q UV irradiation parameters that can be used are an intensity of 40 *W* at a wavelength of 313 *nm*, based on ISO standard 164746. As for the two representative fluids chosen for immersion tests, the Kilfrost immersion temperature could be T = 23°C for a maximal immersion time of 7 *d*, while the Skydrol immersion temperature could be T = 70°C for a maximal immersion time of 48*h*. Thermal treatment parameters that can be used are a temperature, T = 90°C for a time of 100 hours.

### *4.3. Concluding remarks on testing of icephobic coatings*

As a general conclusion to this paragraph it must be stated that novel functional coatings, to which icephobic coatings belong, will be used on future laminar aircraft designs for increasing performance, decreasing fuel consumption, or reducing maintenance. To assess their performance and durability, new test methods must be developed in a common effort among all interested academic, industrial, and regulatory partners. The first outcome of such a joint effort will be harmonized testing guidelines, while the final goal must be to define new industrial standards.

## 5. Hybrid Icephobic coating/active anti-icing and de-icing strategies

Despite the ongoing research efforts on designing and manufacturing icephobic coatings, coatings alone may not be sufficient for aircraft de icing and anti icing needs. In early work carried out by Anderson [101], it was concluded that ice accumulation in an IWTT or in flight conditions is largely dependent upon the external environment, not the surface itself. It went on further to state that as soon as a thin layer of ice was formed, the coating would no longer be functional. There is currently no universal coating solution [102] to resist ice formation under a wide variety of icing conditions and formation modes, including the fully wetted state under the conditions of high speed water droplet (with higher Weber number $We = \rho V^2 R/\gamma$) impingement and condensation from moist environments [6]. Furthermore, many polymer based coatings have shown substantial deterioration after repeated icing/de icing cycles: hydrolysis of fluorooxysilane based coatings (one of the most researched coating bases) contributes to coating degradation; mechanical stresses during icing/de icing cycles compromise the surface asperities [103], hence

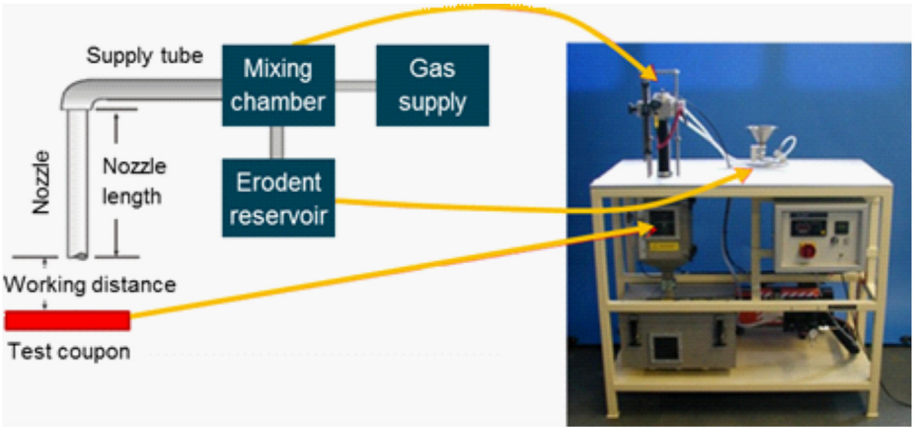


**Fig. 29.** Working principle of the sand erosion test rig Plint TE 68.

the positive function of roughness on wettability; and eventual depletion of lubricants renders the SLIPS system non functional. One of the coating classes detailed 3.3.6 exhibited great promises as a potential anti icing solution as it does not rely on surface micro and nano roughness, nor does it employ an infiltrated lubricant. However, due to the use of elastomer(s) as its matrix, the erosion resistance against sand and ice pellet impact may be poor. In fact, in our preliminary investigation of a commercially available silicone based icephobic coating, it was found that the erosion rate (weight loss) is nearly two orders of magnitude greater than PTFE when being tested under impingement angles of 30° and 45°. Additionally, silica particles (erodent) were observed to have embedded in to the coating surface during the erosion test. In addition to coating durability under harsh conditions, material and process costs and process repeatability prevent some of the coatings and surface modification methods from reaching a commercial maturity stage.

Further to these challenges, the fact holds that as soon as an initial layer of ice or frost forms on the surface, the icephobic property (e.g., impeding ice nucleation/crystallization or rolling off water droplets) will subside and subsequent ice accretion will not be affected by the coating. As such, other means to remove the accreted ice will be needed, even though ice adhesion to the coating may be minimal. To this end, coatings have been found to reduce the power consumption for thermal de icing by 80% while at the same time they decrease runback ice [104]. IWTT of ice adhesion also showed that the best strategy among various methods examined was the combination of electro thermal heating and icephobic coating [105]. Another strategy is to integrate coatings with electro mechanical de icing systems [106].

Each of the following sections briefly reviews existing studies on hybrid de icing systems combining icephobic coatings with thermal or electro mechanical active systems and then gives recommendations to obtain an efficient combination of coatings with either of the three active ice protection systems.

### *5.1. Principles of electro thermal de icing systems and combination of icephobic coatings with electro thermal de icing systems*

#### *5.1.1. Principles of electro thermal de icing systems*

The first investigation of an electro thermal ice protection system goes back to the mid 1930's [107]. The idea is to integrate electrical heating elements into or onto the surface to be protected. These heating elements provide the energy to operate either in anti icing or in de icing mode. Early examples include two designs that were applied to propeller blade protection. The first one consisted of internal wires moulded into a neoprene shoe. The second design used an outer layer of conducting material and an inner isolating layer. Current was supplied to the outer conducting layer via two copper leads. Both designs provided an acceptable ice protection method. However, these concepts had a major drawback: the electro thermal system required a heavy weight electrical generator [108 110].

The arrival of turbojet engines led to some further development of electro thermal technology. Due to the close spacing and motion between rotor and stator, mechanical abrasion would limit ice formation in the initial compressor stages. Icing of this component was therefore deemed secondary. However, the inlet guide vanes became more critical in terms of ice protection. Icing of inlet guide vanes would seriously affect engine performance. Hence, an ice prevention method using electrical heaters was investigated. The heating element consisted of nichrome wires encased into glass cloth and assumed a hairpin shape [111]. It was shown experimentally that power requirements could be significantly reduced, while maintaining ice protection, by operating the heaters in a cyclical activation mode.

With the turbojet engine also came high altitude and high speed flight. Studies showed that the heat required for continuous anti icing of large critical surfaces could become very large, and even prohibitive [112]. In order to reduce the energy penalty required by thermal systems, investigation began on periodic de icing. In this context electro thermal architectures were also investigated [113]. The heating elements consisted of nichrome strips and were placed in the spanwise direction with very little spacing. The strips were integrated into a piling of glass cloth and neoprene. The use of a parting strip was found necessary for quick and complete ice removal. High local power densities and short cycles were also found to yield the best results. However, attaining the melting temperature at the surface was insufficient to ensure ice removal. Peak temperatures of 10 35 °C were found necessary for complete ice removal.

Today, in the context of more electric aircraft and the need to reduce fuel consumption, aircraft manufacturers are showing a growing interest for electro thermal ice protection systems (ETIPS). The fact that Boeing has equipped its 787 *Dreamliner* with an ETIPS demonstrates the degree of maturity this technology has achieved. However, many questions remain to be answered: how does the ice detach in de icing mode? Is there an optimal layout for the heaters? Is it possible to combine an ETIPS with a surface coating to reduce its energy consumption?

The architecture of an ETIPS is usually based on a multi layered stack of materials. Each stack may differ in material properties and thickness depending on the design and applications. The operating of a modern electro thermal ice protection system in de icing mode is illustrated in Fig. 30. A parting strip (here heater C) is held active during

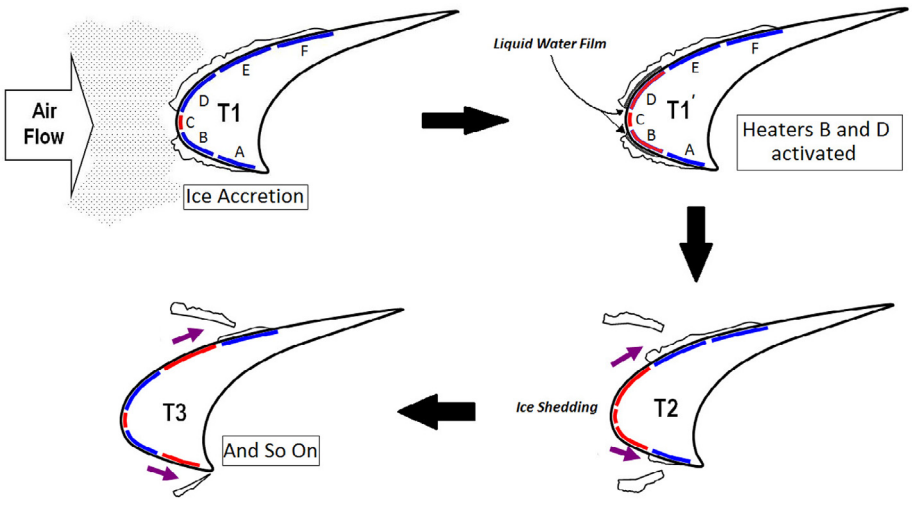


**Fig. 30.** Illustration of an ETIPS operating in de-icing mode.

the whole cycle. The remaining heaters are activated according to a defined cycle. This acts to create a liquid water film at the interface between the ice and the protected surface, hence reducing the ice's ability to remain attached to the surface. Once a critical amount of water film is formed, the ice block is shed under the effect of aero dynamic forces [113].

#### 5.1.2. Combination of coatings with electro thermal systems in anti icing and de icing modes

As a continuation of their earlier experimental studies in 2002 [114], researchers at the Anti icing Materials International Laboratory (AMIL) explored the employment of thermoelectric anti icing systems with hydrophobic coatings [115]. Three different coatings were tested (two hydrophobic and one superhydrophobic). Icing conditions were created using AMIL's icing wind tunnel. The superhydrophobic coating reduced the required power (for noncoated surface) by 13% for rime ice and 33% for glaze ice while the hydrophobic coatings decreased the power by 8% and 13% for rime and glaze ice respectively. However hydrophobic coatings did not prevent runback water from freezing on the unprotected areas. On the other hand, the superhydrophobic coating prevented the runback water from freezing, leaving the surface mostly free of ice. This suggests that a superhydrophobic coating could significantly reduce the power requirement of anti icing systems, al though the question of durability remains to be investigated.

In addition, a study by Antonini et al. investigated the effect of superhydrophobic coatings on energy reduction in anti icing systems [104]. To do so the authors used a NACA0021 aluminum airfoil with an exchangeable insert section. Three different inserts were considered: untreated aluminium, aluminium coated with PMMA and etched alu minium coated with Teflon. The leading edge area was heated with an electrical resistor placed on its inner surface. Moreover, in order to quantify the coating performance, a no ice area was defined on the insert. With this configuration, the heating power needed to keep the no ice area free of ice was measured for different inserts. The perfor mance of a given coating was assessed by measuring the heating power and the amount of runback ice. Tests were performed with LWC's of 1.5 $g/m^3$ and 12.3 $g/m^3$. The airflow velocity and static temperature were 28 m/s and −17 °C respectively. In the first case, it was found that the coated surfaces leaded to a significant reduction of the heating power (up to 80%). A reduction of runback ice was also noted. More over, it was observed that for the Teflon coating, the airfoil remained almost completely free of runback ice. For the second LWC case, the reduction of the heating power was much smaller (10%). However, this value of LWC is not typical of aircraft icing conditions.

Mangini et al. evaluated the effect of hydrophilic and hydrophobic surfaces on runback ice formation [116]. The authors used the same airfoil setup as in the previous study [104]. Two inserts were con sidered: untreated bare aluminium (measured to be hydrophilic) and an etched aluminium superhydrophobic coating. As in the previous study, an electrical heater was placed at the leading edge. Different nozzles were used to generate a dispersed spray (MVD 50 μm, LWC 2.5 $g/m^3$) and a dense spray (MVD 125 μm, LWC 6.5 $g/m^3$). The airflow velocity and static temperature were 14.4 m/s and −17 °C respectively. The study showed two different types of ice build up depending on the coating. In the case of the hydrophilic surface, the droplets impinging at the heated leading edge created a liquid film. The film was observed to separate into ligaments when flowing downstream. Once beyond the heated area, the water froze, leading to ice build up on a large part of the surface. On the other hand, on the superhydrophobic surface, ice only built up as a few isolated islands. Moreover, some of the islands were shed by the aerodynamic forces. The authors hence conclude that superhydrophobic coatings could provide a significant enhancement to thermal ice protection systems.

The previously described studies show that there is a need in further evaluating the performance of an ETIPS combined with surface coat ings. Indeed, a judiciously chosen coating could significantly reduce the energy required to protect a surface from icing. However, the physics of ice formation on surface coatings is complex. No clear standards on their use and effects are available. In fact, studies are usually conducted under low airflow velocities (with respect to large airliners). Information is also lacking on the effect of velocity on the observed physics of ice formation on coated surfaces. Finally, no study has yet attempted to investigate the combination of an ETIPS operating in de icing mode with a coated surface. Therefore, although coatings offer a very promising direction of research for the improvement of ETIPS technology, further work is required in order to fully understand their physics and use them in an optimal way.

### 5.2. Principles of electro mechanical de icing systems and combination of icephobic coatings with electro mechanical de icing systems

In the context of setting up new programmes for more electric air craft and for reducing fuel consumption and emissions, aircraft manu facturers must develop alternative solutions to the traditional thermal

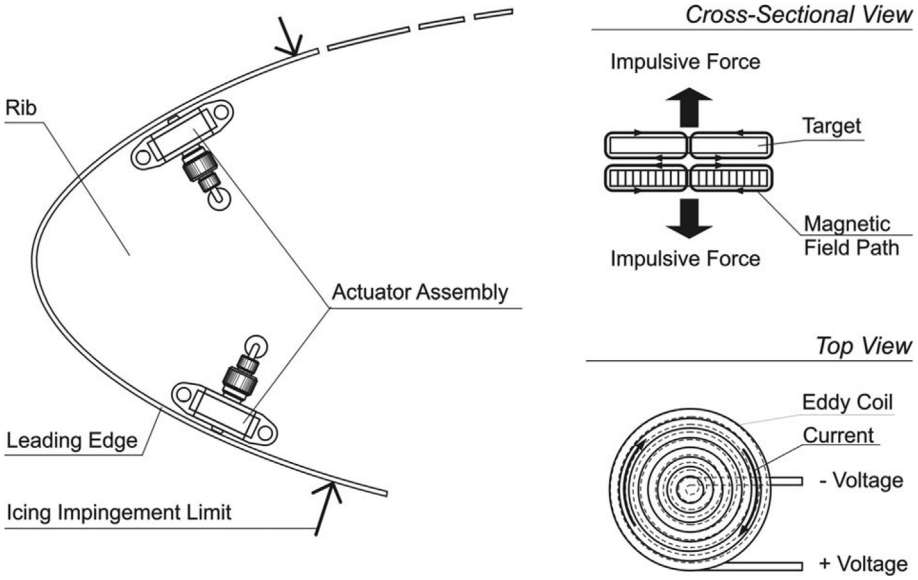


**Fig. 31.** *Schematic of an EIDI system.* Reproduced from Ref. [119].

and pneumatic ice protection systems. In addition to electro thermal ice protection systems, studies are carried out to develop electro mechan ical de icing systems. This technology is at a low maturity stage of re search for de icing purposes, however, it deserves further attention.

*5.2.1. Principles of electro mechanical de icing systems*

The most frequently studied electro mechanical de icing systems are electro impulsive, electro mechanical expulsive, and piezoelectric sys tems.

*5.2.1.1. Electro impulsive de icing systems*. Electro impulsive de icing systems (EIDI) induce de icing by transferring a mechanical impulse to the surface on which the ice has formed. The system operates using high voltage capacitors which are rapidly discharged through electromagnetic coils located under the surface. After the discharge, strong and rapid repulsive magnetic forces are induced from a high current electric pulse through the coil. This results in the rapid acceleration and flexure of the iced surface, causing detachment and shedding of the ice [117,118]. Fig. 31 shows a schematic diagram for an EIDI system. The drawbacks of this technology are the possible induction of structural fatigue, the generation of electromagnetic interference, the non negligible weight of the de icing system, and the disturbing (acoustic) noise generated during de icing.

*5.2.1.2. Electro mechanical expulsive de icing systems*. In electro mechanical expulsive de icing systems (EMED), a short lived electrical pulse delivered to the coils causes them to extend in a few ms [119] and their deformation is transferred to the leading edge. The rapid change of shape of the leading edge results in vibrations at frequencies in the range of a few kHz and detachment of the accreted ice. Fig. 32 shows a schematic of an EMED system. This system was developed by COX Inc [120]. and these systems have drawbacks similar to the electro impulse de icing systems.

*5.2.1.3. Electro mechanical piezoelectric de icing systems*. Electro mechanical piezoelectric de icing systems cause ice delamination by vibrating the surface on which ice has formed [121,122]. Piezoelectric actuators are bonded on the interior of the surface on which ice accretes and can generate vibrations when they are controlled with alternating voltages. A schematic is shown in Fig. 33. The vibrations are of very small amplitudes compared to the previous technologies and induce less

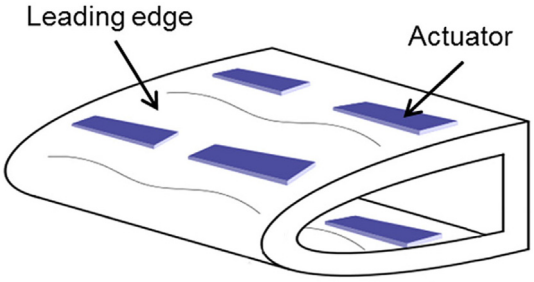


**Fig. 33.** *Schematic of an electro-mechanical piezoelectric de-icing system.* Figure reproduced from Ref. [117] *with permission from Springer.*

structural fatigue. There has been extensive work on this technology, with use of frequencies ranging from hundreds of Hz [117] to tens of kHz [123], to MHz [124].

*5.2.2. Combination of icephobic coatings with electro mechanical de icing systems*

There are very few studies involving hybrid de icing or anti icing systems that combine icephobic coatings and electro mechanical de icing systems. In the work by Strobl, a hybrid system using a coating, heating elements and piezoelectric actuators was proposed and tested in research carried out at Airbus and the Technical University of Munich [125]. A NACA 0012 airfoil was coated and equipped with a thermal system along the stagnation line (in a running wet, anti icing mode) and piezoelectric actuators (cyclically driven for ice shedding) in the unheated aft region, as shown in Fig. 34. The surface was prepared by polishing, anodizing and coating with Episurf solution (Surfactis Technologies, France). A power density of 2.74 kW/m$^2$ was needed to operate the hybrid ice protection system compared to the 16.4 62 kW/ m$^2$ typically required for electro thermal ice protection systems. This clearly showed that by combining various features into an ice protec tion system, the power consumption or the ecological footprint of the active system(s) can be significantly reduced.

Regardless of the electro mechanical de icing technology employed, the ice shedding mechanism is based on vibrations (induced by a shock or by harmonic solicitations) which generate shear stresses greater than the adhesive strength at the interface between ice and substrate, or tensile stress greater than the ice tensile strength. Tensile stress results

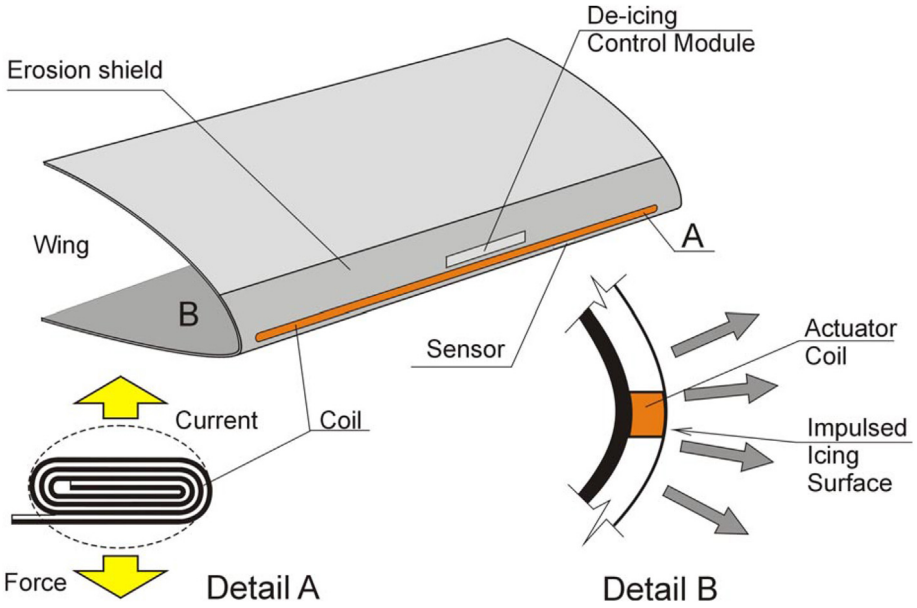


**Fig. 32.** *Schematic of an EMEDS system.* Reproduced from Ref. [119].

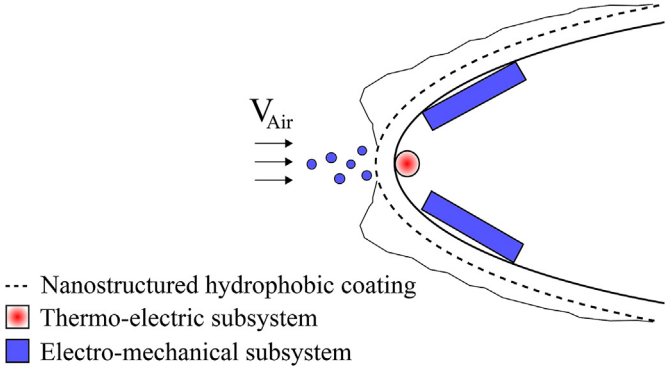


**Fig. 34.** *Illustration of the hybrid ice protection system designed and tested at Airbus.* Figure reproduced from Ref. [125].

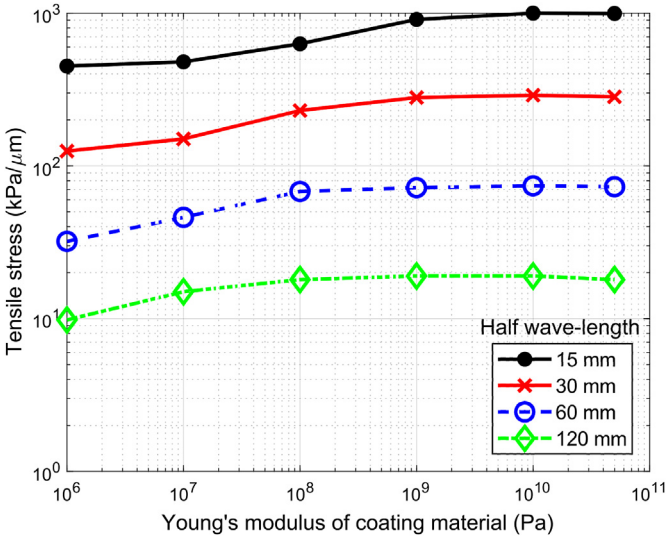


**Fig. 35.** Tensile stress per μm of deformation vs. Young's modulus of the coating for 4 half wave-lengths.

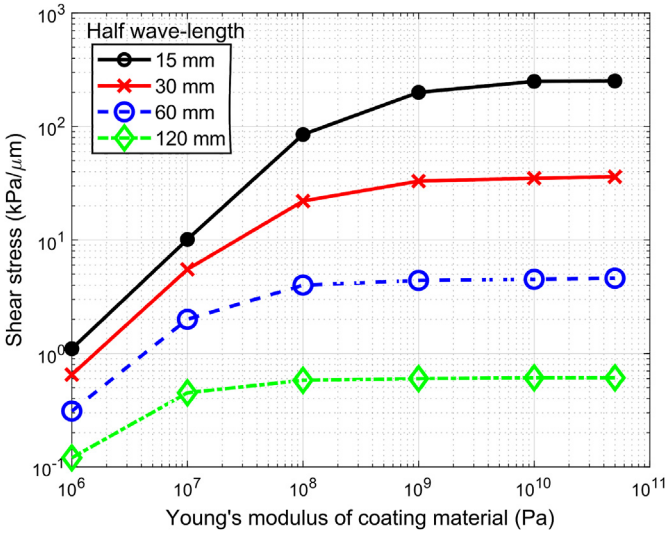


**Fig. 36.** Shear stress per μm of deformation vs. Young's modulus of the coating for 4 half wave-lengths.

in cracks forming within the ice, while shear stress tends to produce delamination. Both phenomena can be used for ice shedding. A decrease in the ice adhesion strength would be beneficial to reduce the electrical power consumption necessary for delamination, provided that the coating does not affect the stress generation. The stress generation is linked to the coupling between the source of vibrations and the ice/substrate interface or the surface layer of the ice. If the coupling is weak, the vibrations are not well transmitted from the source to the substrate and the ice. The coupling and stress generation at the ice/substrate interface or at the surface layer of the ice is strongly dependent on the Young's modulus of the materials, in particular the modulus of the coating. To highlight the effect of the coating, Fig. 35 and Fig. 36 show the change in tensile stress per micron of deformation at the surface layer of the ice and the shear stress per micron of deformation at the ice/substrate interface with respect to the Young's modulus of the coating, respectively. These figures were plotted from simulated results obtained for a 1.5 mm thick aluminium substrate covered with a 100 μm coating layer and a 2 mm thick ice layer (modeled as a homogeneous material with a Young's modulus of 9.33 GPa and a Poisson's ratio of 0.33).

Fig. 35 shows that the tensile stress generated per micron of displacement decreases with Young's modulus. This result is valid for all vibrational frequencies. For shear stress, the same conclusions can be drawn, however, the effects of Young's modulus are more significant. For a coating with a low Young's modulus, the coupling is extremely weak and the shear stress (per micron of displacement) generated at the ice/coating interface is very low. These low stresses imply that a high power would be required to generate a shear stress in excess of the ice adhesion strength in order to remove the ice by delamination, even if the ice adhesion strength has decreased due to the coating.

In order to fully benefit from the icephobicity of a coating combined with an electro mechanical de icing system, we thus recommend using a coating with a Young's modulus that exceeds 1 GPa. If the coating has a lower Young's modulus, the gain obtained from the decrease in ice adhesion strength must be compared to the loss of stress generation to be able to conclude if there is a real benefit of using the coating.

To finalize this section on the combination of icephobic coatings with electro mechanical de icing systems, Table 6 provides the Young's modulus range of the main families of coatings and an assessment of their use for a hybrid icephobic and electro mechanical de icing system.

## 6. Concluding remarks

A summary of the material and surface properties required for coatings to be effective alone or as part of a hybrid de icing system, operating in anti icing or de icing purpose mode is presented in Fig. 37. To achieve the functions of anti icing and de icing, coatings must have the ability to repel water droplets, delay ice nucleation from both vapor and liquid states, and finally once ice is formed on the surface, to reduce ice adhesion. All three characteristics can be realized by (1) coating material selection (fluoro or silicone based), (2) material molecular structure changes (degree of cross link and/or addition of interfacial lubricant), (3) surface morphology/topology changes (creating a texture on the material itself or utilizing micro and nano particles) and addition of infiltrated lubricant/anti freezing agent, and (4) finally changing the surface physical properties such as dielectric constant or polarity. Out of the coatings surveyed, the coating series designed by controlling degree of cross link and the addition of integral interfacial lubricant demonstrated the best performance in terms of anti icing ability, durability and low process cost; however, its effectiveness against all types of icing conditions, its erosion resistance to sand and ice pellets and its adhesion strength to aluminium and composite surfaces are still not tested. In general, a composite structure with micro and/or nano scaled hard particles within a low surface energy polymer matrix may be the solution to look for. Particles can provide the needed mechanical and physical properties, and a venue to impart surface texture.

Despite the effectiveness of the current and future coatings in delaying ice formation and reducing ice adhesion, it will have to work in

**Table 6**
Young's modulus range of the main family of coatings and potential benefit for hybrid coating/electro-mechanical systems.

| Coating type | Young's modulus range | Potential benefit for hybrid coating/electro-mechanical system |
|---|---|---|
| Polymer coatings based on fluoropolymers | 0.5 GPa [133] | - Potential use if the damping is not significant<br>- Erosion may be problematic |
| Polydimethylsiloxane based viscoelastic elastomer coatings | 1–3 MPa [133,134] | - Young's modulus too low to be used in a hybrid system |
| Surface texturing and topology modifications (Al, Ti) | 70–120 GPa [135] | - Surface is the same chemical composition as the substrate<br>- Wear shown not to be an issue |
| CVD/PVD diamond film, TiN | 100–1200 GPa [136–138] | - Thin, wear resistant coatings can be used<br>- Coating application process is expensive |

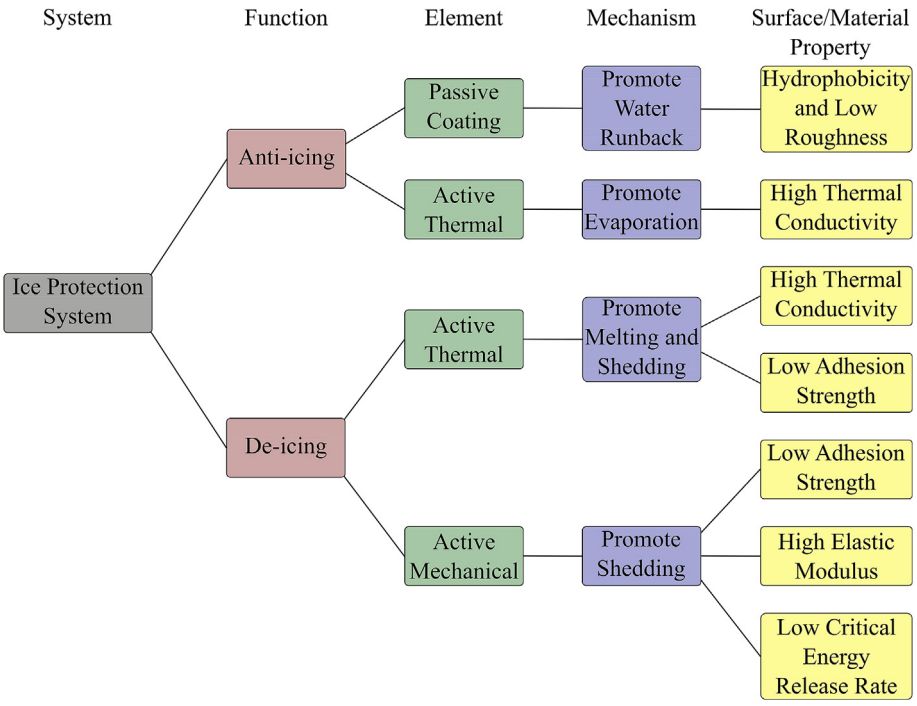


**Fig. 37.** Summary of the material and surface properties required from coatings to achieve anti-icing and de-icing.

concert with active systems to deliver fail safe anti icing and de icing solutions for future aircraft. In this regard, it is foreseeable that heating, vibration or microwave systems may be combined with icephobic coatings to provide the de icing operation, should extended icing con dition result in ice accumulation on critical aircraft components. The energy needed to operate the active system(s) will be greatly reduced due to the presence of the coating. The active system may also assist the coating in preventing ice formation in the first place and avoiding the "ballistic" effect of shedding large pieces of ice during de icing opera tions, i.e. to shed smaller ice fragments at a higher frequency since smaller pieces represent a lower risk for engines or aircraft control elements.

Moving forward, it is in the authors' opinion that future research shall focus on, but is not limited to, the following areas:

(1) Hybrid coating and low energy (or self powered) active systems. These active systems: heating, vibration, or microwave, are to provide the needed de icing capability once ice has accreted. The integration of two or more systems into the aircraft structure will be crucial as the coating and active system shall not adversely impact the structural integrity and aerodynamic performance.
(2) Coating adhesion to various aerospace substrates (aluminium, carbon fibre reinforced polymer (CFRP), glass fibre reinforced polymer (GFRP) and metal composite laminate) should be con sidered as part of the coating development process as its adhesion to surface is as important as the icephobic properties.
(3) Before undertaking extensive icephobic coating development and qualification tests, there is an urgent need to establish international standards (ASTM, ASME, AIAA, SAE or OEMs) to standardize the sample dimensions, coating thickness, coating and ice adhesion tests (test type, strain rate, and environment), and icing test con ditions. More complicated than common mechanical tests, there are a host of icing variables that must be specified, such as sample/ coating temperature and inclination, supercooled water droplet size, velocity and temperature, wind speed (turbulent or laminar), wind tunnel/chamber humidity and temperature. These will allow relative ranking of all coatings and more importantly align coating development for aerospace applications.
(4) Lastly there is a need for standardized environmental testing pro cedures to assess a coating's functional resistance to UV (A and B), de icing chemicals, water/ice, and mechanical abrasion from sand, ice pellets and water droplets in addition to cyclic stresses from aircraft operation, icing/de icing, and vibration.

## Acknowledgement

Dr. Huang would like to thank the Institute of Clement Ader and INSA at University of Toulouse for giving her the opportunities to work with its researchers and exchange valuable ideas.

## References


[1] F.T. Lynch, A. Khodadoust, Effects of ice accretion on aircraft aerodynamics, Prog. Aero. Sci. 37 (2001) 669–767.
[2] Federal Aviation Administration, Advisory Circular No 91-74B: Flight in Icing Conditions, U.S. Department of Transportation, 2015.
[3] R. Ramachandran, M. Kozhukhova, K. Sobolev, M. Nosonovsky, Anti-icing superhydrophobic surfaces: controlling entropic molecular interactions to design novel icephobic concrete, Entropy 18 (2016) 132–158.
[4] S.R. Corsi, S.W. Geis, J.E. Loyo-Rosales, C.P. Rice, R.J. Sheesley, G.G. Failey, C.D. Cancilla, Characterization of aircraft deicer and anti-icer components and toxicity in airport snowbanks and snowmelt runoff, Environ. Sci. Technol. 40 (2006) 3195–3202.
[5] A.I. Freeman, B.W.J. Surridge, M. Matthews, M. Steward, Understanding and managing de-icer contamination of airport surface waters: a synthesis and future perspectives, Environ. Technol. Innov. 3 (2015) 46–62.
[6] A.J. Meuler, G.H. McKinley, R.E. Cohen, Exploiting topographical texture to impart icephobicity, ACS Nano 4 (2) (2010) 7048–7052.
[7] R. Smith-Johannsen, "Surface having low adhesion to ice". United States Patent 2, 617,269, 11 November 1952.
[8] C. Zhang, H. Liu, Effect of drop size on the impact thermodynamics for supercooled large droplet in aircraft icing, Phys. Fluids 28 (2016) 062107.
[9] Y. Lian, Y. Guo, Investigation of the Splashing Phenomenon of Large Droplets for Aviation Safety, SAE Technical Paper 2015-01-2100 (2015).
[10] O. Parent, A. Ilinca, Anti-icing and de-icing techniques for wind turbines: critical Review, Cold Reg. Sci. Technol. 65 (2011) 88–96.
[11] A. Amendola, G. Mingione, On the problem of icing for modern civil aircraft, Air Space Eur. 3 (3/4) (2001) 214–217.
[12] A.G. Kraj, E.L. Bibeau, Phases of icing on wind turbine blades characterized by ice accumulation, Renew. Energy 35 (2010) 966–972.
[13] G. Mingione, M. Barocco, E. Denti, F.G. Bindi, Flight in Icing Conditions, Directorate General for Civil Aviation, 2008.
[14] Aircraft deicing and anti-icing equipment," Safety Adv., no. 2, pp. 1-8.
[15] H. Sojoudi, M. Wang, N.D. Boscher, G.H. McKinley, K.K. Gleason, Durable and scalable icephobic surfaces: similarity and distinctions from superhydrophobic surfaces, Soft Matter 12 (2016) 1938–1963.
[16] S. Nishimoto, B. Bhushan, Bioinspired self-cleaning surfaces with superhydrophobicity, superoleophobicity and superhydrophilicity, RSC Adv. 3 (2013) 671–691.
[17] K.K. Varanasi, T. Deng, M.F. Hsu, N. Bhate, Design of superhydrophobic surfaces for optimum roll-off and droplet impact resistance, Proceedings of the ASME International Mechanical Engineering Congress and Exposition IMECE2008, October 31 - November 6, 2008, Boston, MA, 2008.
[18] K. Varanasi, T. Deng, J.D. Smith, M. Hsu, N. Bhate, frost formation and ice adhesion on superhydrophobic surfaces, Appl. Phys. Lett. 97 (234102) (2010) 1–3.
[19] A.H. Stone, Ice-phobic surfaces that are wet, ACS Nano 6 (8) (2012) 6536–6539.
[20] L. Makkonen, Ice adhesion —theory, measurements and countermeasures, J. Adhes. Sci. Technol. 26 (2012) 413–445.
[21] G. Fortin, Super-Hydrophobic Coatings as a Part of the Aircraft Ice Protection System, SAE Technical Paper 2017-01-2139 (2017).
[22] Y.H. Yeong, J. Sokhey, E. Loth, Ice adhesion on superhydrophobic coatings in an icing wind tunnel, Advances in Polymer Science, Springer, Berlin, Heidelberg, 2017.
[23] S.A. Kulinich, M. Farzaneh, On ice-releasing properties of rough hydrophobic coatings, Cold Reg. Sci. Technol. 65 (2011) 60–64.
[24] S.A. Kulinich, S. Farhadi, K. Nose, X.W. Du, Superhydrophobic surfaces: are they really ice-repellent, Langmuir Lett. 27 (1) (2011) 25–29.
[25] M. Susoff, K. Siegmann, C. Pfaffenroth, M. Hirayama, Evaluation of icephobic coatings - screening of different coatings and influence of roughness, Appl. Surf. Sci. 282 (2013) 870–879.
[26] J. Chen, J. Liu, M. He, K. Li, D. Cui, Q. Zhang, X. Zeng, Y. Zhang, J. Wang, Y. Song, Superhydrophobic surfaces cannot reduce ice adhesion, Appl. Phys. Lett. 101 (2012) 111603.
[27] R.J. Scavuzzo, M.L. Chu, Structural Properties of Impact Ices Accreted on Aircraft Structures, Akron, Ohio, 1987.
[28] G. Momen, R. Jafari, M. Farzaneh, Ice repellency behaviour of superhydrophobic surfaces: effects of atmospheric icing conditions and surface roughness, Appl. Surf. Sci. 349 (2015) 211–281.
[29] V. Hejazi, K. Sobolev, M. Nosonovsky, From superhydrophobicity to icephobicity: forces and interaction analysis, Sci. Rep. 3 (1–6) (2013) 2194.
[30] M. Nosonovsky, V. Hejazi, Why superhydrophobic surface are not always icephobic? ACS Nano 6 (2012) 8488–8491.
[31] S. Farhadi, M. Farzaneh, S.A. Kulinich, Anti-icing performance of superhydrophobic surfaces, Appl. Surf. Sci. 257 (2011) 6264–6269.
[32] A.J. Meuler, J.D. Smith, K.K. Varanasi, J. Mabry, G.H. McKinley, R.E. Cohen, Relationships between water wettability and ice adhesion, ACS Appl. Mater. Interfaces 2 (3100) (2010) 1–10.
[33] A. Dotan, H. Dodiuk, C. Laforte, S. Kenig, The relationship between water wetting and ice adhesion, J. Adhes. Sci. Technol. 23 (2009) 1907–1915.
[34] S.T. Wong, S.H. Kang, S.K.Y. Tang, E.J. Smythe, B.J. Hatton, A. Grinthal, J. Aizenberg, Bioinspired self-repairing slippery surfaces with pressure-stable omniphobicity, Nature 477 (2011) 443–447.
[35] I.A. Ryzhkin, V.F. Petrenko, Physical mechanisms responsible for ice adhesion, J. Phys. Chem. 101 (1997) 6267–6270.
[36] N. Saleema, M. Farzaneh, R.W. Paynter, D.K. Sarkar, Prevention of ice accretion on aluminum surfaces by enhancing their hydrophobic properties, J. Adhes. Sci. Technol. 25 (2011) 27–40.
[37] K. Jha, E. Animo-Danso, S. Bekele, G. Eason, M. Tsige, On modulating interfacial structure towards improved anti-icing performance, Coatings 6 (3) (2016) 1–22.
[38] V.F. Petrenko, S. Peng, Reduction of ice adhesion to metal by using self-assembling monolayers (SAMs), Can. J. Phys. 81 (2003) 387–393.
[39] K. Golovin, S.P.R. Kobaku, D.H. Lee, E.T. DiLoreto, J.M. Mabry, A. Tuteja, Designing durable icephobic surfaces, Adv. Sci. 2 (2016) 1–12.
[40] A. Work, Y. Lian, A critical review of the measurement of ice adhesion to solid substrates, Prog. Aero. Sci. 98 (2018) 1–26.
[41] P. Kim, T.S. Wong, J. Alvarenga, M.J. Kreder, W.E. Adorno-Martinez, J. Aizenberg, Liquid-infused nano-structured surfaces with extreme anti-icing and anti-frosting performance, ACS Nano 6 (8) (2012) 6569–6577.
[42] S. Yang, Q. Xia, L. Zhu, J. Xue, Q. Wang, Q.M. Chen, Research on the icephobic properties of fluoropolymer-based materials, Appl. Surf. Sci. 257 (2011) 4956–4962.
[43] C. Peng, S. Xiang, Z. Yuan, J. Xiao, C. Wang, J. Zeng, Preparation and anti-icing of superhydrophobic PVDF coating on a wind turbine blade, Appl. Surf. Sci. 259 (2012) 764–768.
[44] S. Wang, Y. L, M. Sun, C. Zhang, Q. Yang, X. Hong, Preparation of a durable superhydrophobic membrane by electrospinning poly(vinylidene fluoride) (PVDF) mixed with epoxy-siloxane modified SiO2 nanoparticles, J. Colloid Interface Sci. 359 (2) (2011) 380–388.
[45] B.B. Basu, A.K. Paranthaman, A simple method for the preparation of superhydrophobic PVDF–HMFS hybrid composite coatings, Appl. Surf. Sci. 255 (2009) 4479–4483.
[46] D. Zha, S. Mei, Z. Wang, H. Li, Z. Shi, Z. Jin, Superhydrophobic polyvinylidene fluoride/graphene porous materials, Carbon 49 (2011) 5166–5172.
[47] M. Zou, S. Beckford, R.C. Wei, G. Hatton, M.A. Miller, Effects of surface roughness and energy on ice adhesion strength, Appl. Surf. Sci. 257 (2011) 3786–3792.
[48] H. Li, X. Li, C. Luo, Y. Zhao, X. Yuan, Icephobicity of polydimethylsiloxane-b-poly (fluorinated acrylate), Thin Solid Films 573 (2014) 67–73.
[49] X. Li, Y. Zhao, H. Li, X. Yuan, Preparation and icephobic properties of polymehyltrifluoropropylsiloxane-polyacrylate block copolymers, Appl. Surf. Sci. 316 (2014) 222–231.
[50] J.A. Zigmond, K.A. Pollack, S. Smedley, J.E. Raymond, L.A. Link, A. Pavia-Sanders, M.A. Hickner, K.L. Wooley, Investigation of intricate, amphiphilic crosslinked hyperbranched fluoropolymers as anti-icing coatings for extreme environment, J. Polym. Sci., Part A 54 (2016) 238–244.
[51] S.A. Kulinich, M. Farzaneh, Ice adhesion on super-hydrophobic surfaces, Appl. Surf. Sci. 255 (2009) 8153–8157.
[52] P.F. Rios, H. Dodiuk, S. Kenig, S. McCarty, A. Dotan, The effects of nanostructure and composition on the hydrophobic properties of solid surfaces, J. Adhes. Sci. Technol. 20 (6) (2006) 563–587.
[53] L.F. Mobarakeh, R. Jafari, M. Farzaneh, The ice repellency of plasma polymerized hexamethyldisiloxane coating, Appl. Surf. Sci. (2013) 459–463.
[54] M. Hirayam, Activated poly(hydromethylsiloxane) as novel adhesion promoters for metallic surfaces, J. Adhes. 72 (1) (2000) 51–63.
[55] M.E. Yazdanshenas, K. Shateri-Khalilabad, One-step synthesis of superhydrophobic coating on cotton fabric by ultrasonic irradiation, Ind. Eng. Chem. Res. 52 (2013) 12846–12854.
[56] J. Li, Y. Zhao, J. Hu, L. Shu, X. Shi, Anti-icing performance of a superhydrophobic PDMS/modified nano-silica hybrid coating for insulations, J. Adhes. Sci. Technol. 26 (2012) 665–679.
[57] L. Cao, A.K. Jones, V.K. Sikka, J. Wu, D. Gao, Anti-icing superhydrophobic coatings, Langmuir 25 (21) (2009) 12444–12448.
[58] A.G. Dyachenko, M.V. Borysenko, S.V. Pakhovchyshyn, Hydrophilic/hydrophobic properties of silica surfaces modified with metal oxides and polydimethylsiloxane, Adsorpt. Sci. Technol. 22 (6) (2004) 511–516.
[59] D. Ebert, B. Bhushan, Transparent, superhydrophobic, and wear-resistant coatings on glass and polymer substrates using SiO2, ZnO, and ITO nanoparticles, Langmuir 28 (2012) 11391–11399.
[60] Ames Corp, [Online]. Available: www.amescorp.com.
[61] L.B. Boinovich, A.M. Emelyanenko, Anti-icing potential of superhydrophobic coatings, Mendeleev Commun. 23 (2013) 3–10.
[62] C. Laforte, C. Blackburn, J. Perron, R.J. Aubert, Icephobic coating evaluation for aerospace applications, 55th AIAA/ASME/ASCE/AHS/ASC Structures, Structural Dynamics & Materials Conference, National, 2014.
[63] J. Palacios, D. Wolfe, M. Bailey, J. Szefi, Ice testing of a centrifugally powered pneumatic deicing system for helicopter rotor blades, J. Am. Helicopter Soc. 60 (2015) 1–12.
[64] J. Soltis, J. Palacios, T. Eden, D. Wolfe, Ice adhesion mechanisms of erosion-resistant coatings, AIAA J. 53 (2015) 654–662.
[65] S. Jung, M. Dorrestijn, D. Raps, A. Das, C.M. Megaridis, D. Poulikakos, Are superhydrophobic surfaces best for icephobicity, Langmuir 27 (2011) 3059–3066.
[66] G. Barati Darband, M. Aliofkhazraei, S. Khorsand, S. Sokhanvar, A. Kaboli, Science and engineering of superhydrophobic surfaces: review of corrosion resistance, chemical and mechanical stability, Arab. J. Chem. (2018), https://doi.org/10.1016/j.arabjc.2018.01.013.
[67] D. Spitzner, T. Bergmann, S. Apelt, A. Boucher, H.-P. Wiesmann, Reversible switching of icing properties on pyroelectric polyvenylidene fluoride thin film coatings, Coatings 5 (2015) 724–736.
[68] B.G. Park, W. Lee, J.S. Kim, K.B. Lee, Superhydrophobic fabrication of anodic aluminum oxide with durable and pitch controlled nanostructure, Colloid. Surface. Physicochem. Eng. Aspect. 370 (2010) 15–19.
[69] H. Leese, V. Bhurtun, K.P. Lee, D. Mattia, Wetting behaviour of hydrophilic and

hydrophobic nanostructured porous anodic alumina, Colloid. Surface. Physicochem. Eng. Aspect. 420 (2013) 53–58.
[70] X. Zhang, M. Chen, M. Fu, Impact of surface nanostructure on ice nucleation, J. Chem. Phys. 141 (1–7) (2014) 124709.
[71] D. Arnaldo Del Cerro, G.R.B.E. Romer, A.J. Huis in't Veld, Erosion resistant anti-icing surfaces generated by ultra short laser pulses, Phys. Procedia 5 (2010) 231–235.
[72] A. Steele, B.K. Nayak, A. Davis, M.C. Gupta, E. Loth, Linear abrasion of a titanium superhydrophobic surface prepared by ultrafast laser microtexturing, J. Micromech. Microeng. 23 (2013) 1–8.
[73] D. Ebert, B. Bhushan, Durable lotus-effect surfaces with hierarchical structure using micro- and nano-sized hydrophobic silica particles, J. Colloid Interface Sci. 368 (2012) 584–591.
[74] X. Chen, R. Ma, H. Zhou, X. Zhou, L. Che, S. Yao, Z. Wang, Activating the microscale edge effect in a hierarchical surface for frosting suppression and defrosting promotion, Sci. Rep. 3 (2013) 2525–2532.
[75] P. Eberle, M.K. Tiwari, T. Maitra, D. Poulikakos, Rational nanostructuring of surfaces for extraordinary icephobicity, Nanoscale 6 (2014) 4874–4881.
[76] T.M. Schutzius, S. Jung, T. Maitra, P. Eberle, C. Antonini, C. Stamatopoulos, D. Poulikakos, Physics of icing and rational design of surfaces with extraordinary icephobicity, Langmuir 31 (2015) 4807–4821.
[77] P.W. Wilson, W. Lu, H. Xu, P. Kim, M.J. Kreder, J. Alvarenga, J. Aizenberg, Inhibition of ice nucleation by slippery liquid-infused porous surfaces (SLIPS), Phys. Chem. Chem. Phys. 15 (2) (2013) 581–585.
[78] Y.L. Zhang, H. Xia, E. Kim, H.-B. Sun, Recent developments in superhydrophobic surfaces with unique structural and functional properties, Soft Matter 8 (2012) 11217–11231.
[79] Q. Liu, Y. Yang, M. Huang, Y. Zhou, Y. Liu, X. Liang, Durability of a lubricant-infused electrospray silicon rubber surface as an anti-icing coating, Appl. Surf. Sci. 346 (2015) 68–76.
[80] L. Zhu, J. Xue, Y. Wang, Q. Chen, J. Ding, Q. Wang, Ice-phobic coatings based on silicon-oil-infused polydimethylsiloxane, ACS Appl. Mater. Interfaces 5 (10) (2013) 4053–4062.
[81] Y.H. Yeong, C. Wang, K.J. Wynne, M.C. Gupta, Oil-infused superhydrophobic silicone material for low ice adhesion with long-term infusion stability, ACS Appl. Mater. Interfaces 8 (2016) 32050–32059.
[82] X. Sun, V.G. Damle, S. Liu, K. Rykaczewski, Bioinspired stimuli-responsive and antifreeze-secreting anti-icing coatings, Adv. Mater. Interfaces 2 (1–15) (2015) 1400479.
[83] S. L. Sivas, B. Riegler, R. Thomaier and K. Hoover, "A silicone-based ice-phobic coating for aircraft," [Online]. Available: http://www.thomasnet.com/pdf.php?prid=100944.
[84] NuSil Technology LLC, [Online]. Available: www.nusil.com.
[85] K.K.S. Lau, J. Bico, K.B.K. Teo, M. Chowalla, G.A.J. Amaratunga, W.I. Milne, G.H. McKinley, K.K. Gleason, Superhydrophobic carbon nanotube forests, Nano Lett. 3 (12) (2003) 1701–1705.
[86] Y.C. Jung, B. Bhushan, Mechanically durable carbon nanotube-composite hierarchical structures with superhydrophobicity, self-cleaning, and low-drag, ACS Nano 3 (12) (2009) 4155–4163.
[87] A.O. Raji, T. Varadhachary, K. Nan, T. Wang, J. Lin, J. Y, B. Genorio, Y. Zhu, C. Kittrell, J.M. Tour, Composites of graphene nanoribbon stacks and epoxy for joule heating and deicing of surfaces, ACS Appl. Mater. Interfaces 8 (2016) 3551–3556.
[88] V. Volman, Y. Zhu, A.O. Raji, B. Genorio, W. Lu, C. Xiang, C. Kittrell, J.M. Tour, Radio-frequency-transparent, electrically conductive graphene nanoribbon thin film as deicing heating layers, Appl. Mater. Interfaces 6 (2014) 298–304.
[89] Fraunhofer Institute IFAM , "Anti-icing coatings and de-icing technical approaches and status," [Online]. Available: http://windren.se/WW2013/52 Sell Stephan Winterwind 2013.pdf.
[90] T. Wang, Y. Zheng, A.O. Raji, Y. Li, W.K.A. Sikkema, J.M. Tour, Passive anti-icing and active deicing films, ASC Appl. Mater. Interfaces 8 (2016) 14169–14173.
[91] T.V. Charpentier, A. Neville, P. Milner, R.W. Hewson, A. Morina, Development of anti-icing materials by chemical tailoring of hydrophobic textured metallic surfaces, J. Colloid Interface Sci. 394 (2013) 539–544.
[92] G.D. Bixler, B. Bhushan, Bioinspired micro/nanostructured surfaces for oil drag reduction in closed channel flow, Soft Matter 9 (2013) 1620–1635.
[93] Y.C. Jung, B. Bhushan, Biomimetic structures for fluid drag reduction in laminar and turbulent flows, J. Phys. Condens. Matter 22 (2010) 35104–35113.
[94] M.I. Gibson, Slowing the growth of ice with synthetic macromolecules: beyond antifreeze(glyco) proteins, Polym. Chem. 1 (8) (2010) 1141–1152.
[95] Regulation (EC) No 1907/2006 of the European Parliament and of the Council of 18 December 2006 Concerning the Registration, Evaluation, Authorisation and Restriction of Chemicals (REACH), Establishing a European Chemicals Agency, (2006).
[96] A. Heinrich, R. Ross, G. Zumwalt, J. Provorse, V. Padmanabhan, J. Thompson, J. Riley, Aircraft Icing Handbook vol. 3, Gates Learjet Corporation, 1991.
[97] M.L. Toulouse, R. Lewis, A350XWB icing certification overview, AE 2015 International Conference on Icing of Aircraft, Engines, and Structures, 2015.
[98] ISO 2409, Paints and Varnishes - Cross-Cut Test, (2013).
[99] Defence Standard 00-35 Environmental Handbook for Defence Material: Part 4: Natural Environments, (2006) Glasgow.
[100] Standard Test Method for Conducting Erosion Tests by Solid Particle Impingement Using Gas Jets, ASTM G76-13, New York, 2013.
[101] D.N. Anderson, A.D. Reich, Tests of the performance of coatings for low ice adhesion, 35th Aerospace Sciences Meeting and Exhibit, Reno, Nevada, USA, 1997.
[102] A. Alizadeh, V. Bahadur, A. Kulkarni, M. Yamada, J.A. Ruud, Hydrophobic surfaces for control and enhancement of water phase transitions, Interf. Mater. Spec. Wettabil. 38 (5) (2013) 407–411.
[103] L.B. Boinovich, A.M. Emelyanenko, V.K. Ivanov, A.S. Pashinin, Durable icephobic coating for stainless steel, ACS Appl. Mater. Interfaces 5 (2013) 2549–2554.
[104] C. Antonini, M. Innocenti, T. Horn, M. Marengo, A. Amirfazli, Understanding the effect of superhydrophobic coatings on energy reduction in anti-icing system, Cold Reg. Sci. Technol. 67 (2011) 58–67.
[105] A. Kraj, E.L. Bibeau, Measurement method and results of ice adhesion force on the curved surface of a wind turbine blade, Renew. Energy 35 (2010) 741–746.
[106] V. Pommier-Budinger, M. Budinger, N. Tepylo and X. Huang, "Analysis of piezoelectric ice protection systems combined with ice-phobic coatings," in 8th AIAA Atmospheric and Space Environments Conference, Washington, DC, USA, 13-17 June 2016.
[107] Comité d'Etude du Givrage, Rapport du 19 Mai 1938. Bulletin des Services Techniques vol. 85, Publication Scientifiques et Techniques du Ministère de l'Air, 1939.
[108] J.L. Orr, Interim Report on Flight Tests of Thermal-Electric Propeller De-icing. Report MD-25, National Research Council of Canada, 1942.
[109] R. Scherrer, An Analytical Investigation of Thermal-Electric Means of Preventing Ice Formations on a Propeller Blade. Advance Confidential Report 4H31, NACA, 1944.
[110] R. Scherrer, L.A. Rodert, Tests of Thermal-Electric De-icing Equipment for Propellers. Advance Restricted Report 4A20, NACA, 1944.
[111] U. von Glahn, R.E. Blatz, Investigation of Power Requirements for Ice Prevention and Cyclical De-icing of Inlet Guide Vanes with Internal Electric Heaters. Research Memorandum E50H29, NACA, 1950.
[112] T.F. Gelder, J.P. Lewis, S.L. Koutz, Ice Protection for a Turbojet Transport Airplane: Heating Requirements, Methods of Protection and Performance Penalties. Technical Note 2866, NACA, 1953.
[113] J.P. Lewis, D.T. Bowden, Preliminary Investigation of Cyclic De-icing of an Airfoil Using an External Electric Heater. Research Memorandum E51J30, NACA, 1952.
[114] C. Laforte, J.L. Laforte, J.C. Carrier, How a solid coating can reduce the adhesion of ice on a structure, International Workshop on Atmospheric Icing of Structures, Brno, Czech Republic, 2002.
[115] G. Fortin, M. Adomou, J. Perron, Experimental study of hybrid anti-icing systems combining thermoelectric and hydrophobic coatings, SAE 2011 International Conference on Aircraft and Engine Icing and Ground Deicing, Chicago, Illinois, 2011.
[116] D. Mangini, C. Antonini, M. Marengo, A. Amirfazli, Runback ice formation mechanism on hydrophilic and superhydrophobic surfaces, Cold Reg. Sci. Technol. 109 (2015) 53–60.
[117] M. Endres, H. Sommerwerk, C. Mendig, M. Sinapius, P. Horst, Experimental study of two electro-mechanical de-icing systems applied on a wing section tested in an icing wind tunnel, CEAS Aeronaut. J. 8 (3) (2017) 429–439.
[118] C.C. Ryerson, Assessment of Superstructure Ice Protection as Applied to Offshore Oil Operations Safety, (2009) Hanover, New Hampshire.
[119] Z. Goraj, An overview of the deicing and anti-icing technologies with prospects for the future, 24th International Congress of the Aeronautical Science, ICAS, 2004, pp. 1–11 2004.
[120] Cox & Company Inc., "Low Power Ice Protection Systems".
[121] Valérie Pommier-Budinger, Marc Budinger, Pierrick Rouset, Fabien Dezitter, Florent Huet, Marc Wetterwald, Elmar Bonaccurso, Electromechanical resonant ice protection systems: initiation of fractures with piezoelectric actuators, AIAA J. 56 (11) (2018) 4400–4411.
[122] Marc Budinger, Valérie Pommier-Budinger, Lokman Bennani, Pierrick Rouset, Elmar Bonaccurso, Fabien Dezitter, Electromechanical resonant ice protection systems: analysis of fracture propagation mechanisms, AIAA J. 56 (11) (2018) 4412–4422.
[123] A. Overmeyer, J. Palacios, E. Smith, Ultrasonic de-icing bondline design and rotor ice testing, AIAA J. 51 (12) (2013) 2965–2976.
[124] M.K. Kalkowski, T.P. Waters, E. Rustighi, Removing surface accretions with piezo-excited high-frequency structural waves, Active and Passive Smart Structures and Integrated Systems, San Diego, CA, USA, 2015.
[125] T. Strobl, S. Storm, M. Kolb, J. Haag, M. Hornung, Development of a hybrid ice protection system based on nanostructure hydrophobic surfaces, ICAS Conference, St Petersburg, Russia, 2014.
[126] Icing Research Tunnel | NASA Glenn Research Center, NASA 14 (Nov. 2018), www1.grc.nasa.gov/facilities/irt/.
[127] M. Nosonovsky, B. Bhushan, Roughness optimization for biomimetic superhydrophobic surfaces, Microsyst. Technol. 11 (7) (2005) 535–549.
[128] Laboratory Ice Adhesion Test Results for Commercial Icephobic Coatings for Pratt & Whitney, CRREL, May 2004.
[129] Y. Zheng, X. Gao, L. Jiang, Directional adhesion of superhydrophobic butterfly wings, Soft Matter 3 (2007) 178–182.
[130] Federal Aviation Administration, Chapter 15. Ice and rain protection, Aviation Maintenance Technician Airframe Handbook, vol. 2, U.S. Department of Transportation, Washington D.C., 2012.
[131] J. T. Salisbury, "Microwave deicing and anti-icing system for aircraft". United States Patent 5615849 A, 1 April 1997.
[132] C. Yin, Z. Zhang, Z. Wang, H. Guo, Numerical simulation and experimental validation of ultrasonic de-icing system for wind turbine blade, Appl. Acoust. 114 (2016) 19–26.
[133] R.F. Brady, A fracture mechanical analysis of fouling release from nontoxic antifouling coatings, Prog. Org. Coating 43 (1) (2001) 188–192.
[134] I.D. Johnston, D.K. McCluskey, C.K.L. Tan, M.C. Tracey, Mechanical characterization of bulk Sylgard 184 for microfluidics and microengineering, J. Micromech.

Microeng. 24 (3) (2014).
[135] J.R. Davis, Metals Handbook Desk Edition, second ed., ASM International, 1998.
[136] S. Constantinescu, L. Orac, Mechanical properties of TiN thin films investigated using macromachining techniques, 19th International Conference on Metallurgy and Materials, Roznov pod Radhostem, Czech Republic, 2010.
[137] S.H. Kim, H. Park, K.H. Lee, S.H. Jee, D.-J. Kim, Y.S. Yoon, H.B. Chae, Structure and mechanical properties of titanium nitride thin films grown by reactive pulsed laser deposition, J. Ceram. Process. Res. 10 (1) (2009) 49–53.
[138] C.A. Klein, G.F. Cardinale, Young's modulus and Poisson's ratio of CVD diamond, Diam. Relat. Mater. 2 (1993) 918–923.